USING AN OPTICAL SENSOR OF SYNAPTIC VESICLE EXOCYTOSIS TO INVESTIGATE THE RELATIONSHIP BETWEEN RELEASE PROBABILITY AND PAIRED-PULSE PLASTICITY AT INDIVIDUAL HIPPOCAMPAL SYNAPSES

by

Kristen Michelle Chafe

Submitted in partial fulfilment of the requirements
for the degree of Master of Science

at

Dalhousie University
Halifax, Nova Scotia
April 2015

TABLE OF CONTENTS

LIST OF FIGURES

ABSTRACT

Release probability (P_r) is a determinant of synaptic strength that varies considerably between synapses, and correlates with the size of the readily releasable pool (RRP) of synaptic vesicles. Short-term plasticity is quantified in electrophysiological experiments by measuring the paired-pulse ratio (PPR) of postsynaptic current amplitudes in response to two successive stimuli. An inverse relationship has been reported between population-averaged values of P_r and PPR, but this relationship has not yet been examined at the level of individual release sites. We utilized a genetically encoded fluorescent sensor to directly measure P_r, PPR, and RRP size at synapses in dissociated cultures of rat hippocampal neurons. We propose that processes affecting vesicular release probability, i.e. the likelihood that individual synaptic vesicles in the RRP undergo exocytosis, inversely alter P_r and PPR. In contrast, mechanisms modulating the number of synaptic vesicles in the RRP may regulate P_r without affecting PPR. Our findings suggest that the reliability and short-term plasticity of neurotransmitter release can be independently regulated at presynaptic specializations to fine-tune the strength and temporal integration of synaptic transmission.

LIST OF ABBREVIATIONS USED

aa	Amino Acid
AMPA	α-Amino-3-hydroxy-5-methyl-4-isoxazolepropionic Acid
AMPAR	α-Amino-3-hydroxy-5-methyl-4-isoxazolepropionic Acid Receptor
AP	Action Potential
APV	2-amino-5-phosphonovaleric acid
AZ	Active Zone
BFP	Blue Fluorescent Protein
Ca^{2+}	Calcium
CA1	Cornus Ammonis 1
CA3	Cornus Ammonis 3
$CaCl_2$	Calcium Chloride
CaMKII	Calcium/Calmodulin Kinase II
cDNA	Complementary Deoxyribonucleic Acid
CMV promoter	CytoMegalovirus promoter
CO_2	Carbon Dioxide
DNA	Deoxyribonucleic Acid
DNQX	6,7-dinitroquinoxaline-2,3-dione
E18	Embryonic Day 18
EGFP	Enhanced Green Fluorescent Protein
EGTA	Ethylene Glycol Tetraacetic Acid

EPSC	Excitatory Postsynaptic Current
EPSCaT	Excitatory Postsynaptic Calcium Transient
FM1-43	*N*-(3-triethylammoniumpropyl)-4-(4-(dibutylamino)Styryl) Pyridinium Dibromide
fps	Frames per Second
HBS	Hepes Buffered Saline
Hepes	4-(2-hydroxyethyl)-1-piperazineethanesulfonic acid
KCl	Potassium Chloride
KD	Knockdown
LTD	Long-Term Depression
LTP	Long-Term Potentiation
mEPSC	Mini Excitatory Postsynaptic Current
$MgCl_2$	Magnesium Chloride
Na^+	Sodium
NaCl	Sodium Chloride
Na_2HPO_4	Disodium Phosphate
NMDA	N-methyl-D-aspartate
NMDAR	N-methyl-D-aspartate Receptor
NSF	N-ethylmaleimide sensitive fusion proteins
nt	Nucleotide
PPD	Paired-Pulse Depression
PPF	Paired-Pulse Facilitation
PPR	Paired-Pulse Ratio

PPR_E	Paired-Pulse Ratio of Exocytosis
P_r	Release Probability
PSC	Postsynaptic Current
PSD	Postsynaptic Density
PSP	Postsynaptic Potential
ROI	Region of Interest
RRP	Readily Releasable Pool
RT-PCR	Reverse Transcription Polymerase Chain Reaction
SD	Standard Deviation
SEM	Standard Error of the Mean
shRNA	Small Hairpin Ribonucleic Acid
STP	Short-Term Plasticity
SV	Synaptic Vesicle
sypHl	Synaptophysin-pHluorin
TTX	Tetrodotoxin
VGCC	Voltage-Gated Calcium Channel
vP_r	Vesicular Release Probability
$\overline{vP_r}$	Mean Vesicular Release Probability
ΔF	Change in Fluorescence
$\Delta F(1AP)$	Change in Fluorescence After 1 AP
$\Delta F(2AP)$	Change in Fluorescence After 2 APs
$\Delta F(80AP,40Hz)$	Change in Fluorescence After Train of 80 APs at 40Hz

ACKNOWLEDGEMENTS

First and foremost, I would like to express my immense gratitude to my supervisor, Dr. Stefan Krueger, who guided me with patience and expertise through my research project and the writing of my thesis. His excellent mentorship and encouragement over the course of my degree have pushed me to become a more focused and independent researcher.

I would also like to thank Annette Kolar for tirelessly providing the lab with cell cultures, and for sharing her technical expertise and advice, and Dylan Quinn for his much appreciated support and assistance in overcoming obstacles in my work.

I wish to acknowledge the members of my supervisory committee, Dr. Steven Barnes, Dr. Kazue Semba, Dr. Alan Fine, for generating helpful discussion and for providing me with excellent feedback on my project.

Last, but not least, I'd like to thank my boyfriend, Ian Burkovskiy, and my family for their continuous motivation, encouragement, and optimism, throughout my degree.

CHAPTER 1: INTRODUCTION

1.1 SYNAPTIC STRENGTH

Synaptic strength is a measure of how effectively an action potential in the presynaptic bouton is translated into a change in the postsynaptic potential (PSP). Synapses vary in strength due to presynaptic differences in neurotransmitter release and in the sensitivity of the postsynaptic neuron to neurotransmitter. Diversity in strength among synapses has been studied extensively at glutamatergic synapses, particularly in the hippocampus, where they are believed to play a key role in the processes of learning and memory (Scoville and Milner, 1957; Bliss and Lømo, 1973).

1.1.1 Postsynaptic Determinants of Synaptic Strength

A large body of experimental evidence suggests that variability in synaptic strength arises through several postsynaptic mechanisms operating at different scales, including differences in the conductance or density of postsynaptic receptors, differences in synapse size, and the elimination of existing synapses or the formation of new ones.

The postsynaptic density (PSD) is a protein-dense structure that lies in close proximity to the synaptic membrane (Harris and Stevens, 1989) and contains the synapse's neurotransmitter receptors and scaffolding proteins. Synapses vary in their expression of several PSD components, including, most importantly, the α-amino-3-hydroxy-5-methyl-4-isoxazolepropionic acid (AMPA) ionotropic glutamate receptor. The postsynaptic localization of AMPA receptors (AMPARs) is highly plastic and is a determinant of synaptic strength. This has been clearly demonstrated by the unmasking of silent synapses, which do not contain functional AMPARs (Kullmann et al., 1994; Liao et

al., 1995; Isaac et al., 1995). Silent synapses contain only N-methyl-D-aspartate receptors (NMDARs) and are unresponsive to presynaptic neurotransmitter release due to a blockade of the NMDAR channel pore by magnesium ions when the postsynaptic neuron is at resting membrane potential. Silent synapses are common in early mammalian development, and a gradual increase in responsiveness for hippocampal CA1 synapses over time (Hsia et al., 1998) has been shown to correlate with AMPAR insertion at the PSD (Petralia et al., 1999). Silent synapses are unmasked in response to temporally correlated pre- and postsynaptic activity, which leads to the insertion of AMPARs and results in the long-term potentiation (LTP) of synaptic strength (Isaac et al., 1995; Liao et al., 1995; Isaac et al., 1996; Shi et al., 1999).

The increase in synaptic strength that follows LTP induction at Schaffer collateral synapses in the hippocampus has been shown to reflect not only a change in AMPAR density, but also in AMPAR single channel conductance (Benke et al., 1998). Changes in AMPAR conductance appear to rely on CaMKII-dependent phosphorylation of the GluA1 AMPAR subunit (Derkach et al., 1999; Kristensen et al., 2011) which has been shown to occur following a chemically-induced modulation of synaptic strength (Lee et al., 1998).

Another potential determinant of synaptic strength is the size of the synapse itself. Thin protrusions from the dendritic shaft of glutamatergic neurons called spines have been observed to undergo activity-induced changes in diameter which correlate with changes in synaptic strength (Matsuzaki et al., 2004; Zhou et al., 2004; Yuste et al., 2014). This is likely due to the fact that the size of a spine is proportional to the size of the PSD that it contains (Harris and Stevens, 1989; Meyer et al., 2014). Therefore,

activity-induced changes in spine size correlate with changes in PSD length (Desmond and Levy, 1986), leading to an increase in space that is available for postsynaptic AMPARs (Kopec et al., 2007). As previously mentioned, AMPAR density is a major determinant of synaptic strength.

Finally, it has been observed that the induction of synaptic plasticity in CA1 pyramidal neurons is associated with a change in the total number of synapses in the preparation. An increase in synaptic strength correlates with an increase in the density of protrusions along the dendritic shaft, which will eventually develop into functional spines and form new synapses (Maletic-Savatic et al., 1999; Engert and Bonhoeffer, 1999). Likewise, a reduction in synaptic strength leads to a decrease in spine density in hippocampal slice cultures (Nägerl et al., 2004), demonstrating that there is a bidirectional process by which the formation of new synapses, or elimination of existing synapses, may regulate synaptic plasticity.

1.1.2 Presynaptic Determinants of Synaptic Strength

Neurotransmitter release probability is a highly variable factor of synaptic strength

Not every action potential elicits neurotransmitter release (Allen and Stevens, 1994; Stevens and Wang, 1995). An increased likelihood of release at a particular synapse may contribute to an increase in synaptic strength because it allows that synapse to make a larger contribution to the generation of a PSP. Synaptic reliability is discussed in terms of release probability (P_r), which is the probability that exocytosis will occur in response to a single action potential.

There is a great deal of variability between the release probabilities of different synaptic populations. For example, climbing fibre synapses onto Purkinje cells tend to have a high release probability when stimulated from rest (P_r = 0.90, Silver et al., 1998), whereas parallel fibre synapses onto Purkinje cells show a low average release probability (P_r = 0.05, Dittman et al., 2000). An intermediate release probability is found in populations of Schaffer collateral synapses onto CA1 cells (P_r = 0.24 – 0.3; Allen and Stevens, 1994, Dittman et al., 2000) as well as inhibitory neurons in rat hippocampal cell culture (P_r = 0.34, Baldelli et al., 2005) and the Calyx of Held synapses in brainstem slices (P_r = 0.25-0.40, Meyer et al., 2001). P_r has also been demonstrated to vary within populations. For example, a 6-fold difference in release probability has been measured among synapses in hippocampal slice cultures (Hessler et al., 1993). Interestingly, the use of styryl dyes to measure neurotransmitter release at individual release sites has revealed that P_r may vary considerably even between the synapses of a single cell, ranging from 0.05 to 0.9 at the release sites of a single hippocampal neuron (Murthy et al., 1997; Branco et al., 2010).

Release probability is regulated by synapse size

An active zone (AZ) is a presynaptic specialization that contains the machinery required to elicit neurotransmitter release. It contains structural proteins, neurotransmitter-containing vesicles, and voltage-gated calcium channels (VGCCs; Südhof, 2012). In hippocampal neurons, where the size of the AZ has been assessed at individual synapses using electron microscopy and immunolabeling of cytomatrix proteins, synapses with large AZs are more likely to have a high P_r than synapses with

small AZs (Matz et al., 2010; Holderith et al., 2012). This may be due to the fact that larger AZs are able to accommodate a greater number of synaptic vesicles (SVs) for immediate release.

The size of the AZ has been shown to correlate with the size of the docked vesicle pool, which is made up of the portion of SVs that are in close contact with the neuronal membrane (Schikorski and Stevens, 1997; Murthy et al., 2001; Matkovic et al., 2013). The size of the docked vesicle pool, in turn, correlates with P_r (Murthy et al., 1997). The readily releasable pool (RRP) is thought to be an even smaller vesicle pool that contains only the subset of docked vesicles that are available to be released quickly in response to calcium influx. The size of the RRP correlates with the total number of docked vesicles (Schikorski and Stevens, 2001) and is predictive of P_r (Murthy et al., 2001; Branco et al., 2010; Dobrunz and Stevens, 1997). Spontaneous changes in AZ size that occur in cultured hippocampal neurons have been associated with changes in both RRP size and P_r at those synapses (Matz et al., 2010), providing evidence that AZ size is associated with P_r through changes in the size of the readily-releasable vesicle pool.

The size of the AZ appears to be co-regulated along with the size of the PSD (Pierce and Mendell, 1993; Schikorski and Stevens, 1997). Pharmacologically induced network inactivity has been shown to cause increases in both AZ size and PSD size, as well as increasing the size of the RRP and the P_r of the synapse (Murthy et al., 2001). Selective overexpression of exogenous PSD-95, a scaffolding protein that is abundant in the PSD, increases the number of vesicles in the presynaptic specialization (El-Husseini et al., 2000) and enhances P_r (Futai et al., 2007). It therefore seems possible that P_r can be

indirectly modulated by the size of the PSD through trans-synaptic changes to the active zone.

Neurotransmitter release requires docking and priming of synaptic vesicles

The RRP is defined as the portion of SVs that are both docked and primed, and are therefore available for fast release when an AP arrives at the axon terminal. After docking occurs, the priming step organizes vesicles into the correct position to be exocytosed in response to calcium influx. This is done through the formation of a soluble NSF attachment protein receptor (SNARE) complex - an interaction between synaptobrevin, which is a protein embedded in the vesicular membrane, and syntaxin as well as SNAP-25, proteins localized to the presynaptic cell membrane. The assembly of the SNARE complex forces the two membranes to be in close apposition to each other so exocytosis can be initiated quickly when calcium enters the synaptic terminal. The enhancement of SNARE complex assembly may influence synaptic strength by increasing the size of the readily releasable pool of SVs (Augustin et al., 1999, Betz et al., 2001) or by increasing the apparent calcium sensitivity of exocytosis (Acuna et al., 2014).

The unfolding of syntaxin is a critical regulatory event in vesicle priming, because syntaxin is only able to bind to other SNARE proteins in its open conformation (Richmond, 2001; Zilly et al., 2006). The unfolding of syntaxin may be facilitated by Munc-13 (Augustin et al., 1999; Richmond et al., 2001; McEwen et al., 2006) or by Munc-18 (Hata et al., 1993; Zilly et al., 2006). Binding between syntaxin and Munc18 is an important regulatory step of vesicle exocytosis to such an extent that mice lacking Munc-18 show a complete loss of neurotransmitter release at all synapses (Verhage et al.,

2000).

Regulation of synaptic release probability by calcium influx and vesicle fusion

P_r is strongly regulated by modulation of calcium influx through VGCCs. When the flow of calcium into the presynaptic terminal increases, the likelihood of triggering calcium-dependent exocytosis also increases. As outlined in detail in the following section, alterations in calcium-triggered synaptic vesicle exocytosis may result from differences in the density of VGCCs at each AZ, differences in channel conductances, or differences in the spatial co-ordination between SVs and calcium channels.

The number of presynaptic calcium channels varies dramatically between synapses. At the Calyx of Held, each AZ has between 5-218 VGCCs, and a higher number of channels corresponds to a larger P_r (Sheng et al., 2012). Neurons that lack the presynaptic protein RIM show both reduced calcium channel density and diminished neurotransmitter release (Kaeser et al., 2011; Han et al., 2011) while cells expressing the α2δ calcium channel subunit exhibit increased VGCC density as well as increased release probability (Hoppa et al., 2012). It therefore seems likely that VGCC density at the synapse is a regulator of release probability.

In addition to alterations in the density of presynaptic calcium channels, changes in their conductance may also play a role in modulating release probability. Calcium sensor proteins, such as calmodulin, have been shown to influence conductance of P/Q type calcium channels. Calcium-calmodulin binding to P/Q-type VGCCs enhances the amount of calcium that is able to enter the presynaptic terminal (Lee et al., 1999). Mutations that prevent such interactions between VGCC and calcium sensor proteins

suppress activity-dependent changes in the release probability of cultured synapses (Mochida et al., 2008), demonstrating that a modulation of channel conductance is sufficient to produce changes in P_r. In addition, the activation of G-proteins reduces calcium influx following the application of noradrenaline or GABA (Dunlap and Fischbach, 1978; Holz et al., 1986) by changing the voltage-dependence of calcium channels (Bean, 1989). Therefore, G-protein activation is another potential mechanism by which signalling molecules might modulate calcium current, and consequently P_r, through changes in VGCC conductance.

For efficient neurotransmitter release, calcium ions must trigger exocytosis before they are sequestered by endogenous calcium buffers. Close spatial coordination between primed synaptic vesicles and VGCCs is therefore essential so that the calcium ions may bind quickly to the vesicular calcium sensor protein synaptotagmin and rapidly trigger release. The spatial co-ordination between VGCCs and vesicles varies between synapses, and undergoes changes at central synapses during typical mammalian development (Cao et al., 2010; Yang et al., 2010; Eggermann et al., 2012). The spatial coupling is loose in early development, but tightens during maturation (Fedchyshyn and Wang, 2005). In adult rat brainstem slices, the composition of a VGCC has an influence on its coupling to SVs (Wu et al., 1999). For example, recent evidence suggests that expression of the α2δ VGCC subunit increases P_r in hippocampal neurons by tightening the interaction between VGCC and synaptic vesicles (Hoppa et al., 2012).

Methods of measuring release probability

Electrophysiology is an indirect, but commonly used, method of estimating release probability. The amplitude of the average postsynaptic potential (PSP) or postsynaptic current (PSC) recorded over many trials is proportional to P_r. However, as previously discussed, the PSP or PSC amplitude is also influenced by postsynaptic mechanisms such as the AMPAR density and conductance. For this reason, more specific electrophysiological methods have been developed to assess presynaptic release. One approach is to bathe synapses in solution containing the irreversible, activity-dependent NMDAR-channel blocker, MK-801, while obtaining a whole-cell recording of the postsynaptic cell. The rate of decline of the NMDAR-mediated current in response to spontaneous presynaptic activity can then be used to estimate the rate of presynaptic release events (Rosenmund et al, 1993). This method provides an average P_r value for a population of synapses. If it is used to compare P_r values of a population before and after a pharmacological or genetic manipulation, it relies on the assumption that the manipulation does not affect synaptic density or conductance of NMDARs, since these factors may also affect the rate of the NMDAR block independently of changes in P_r. Other electrophysiological methods include the use of mEPSC frequency as an estimate of the number of spontaneous presynaptic release events, and minimal stimulation, during which the strength of the extracellular stimulation is adjusted to very low intensities to assess the rate of neurotransmission failures and thus obtain an estimate of P_r. Finally, paired-pulse plasticity is often assessed in lieu of measuring release probability directly. I will revisit this technique in my discussion of short-term plasticity. For each of the electrophysiological methods addressed thus far, even a single afferent neuron that is

stimulated may contribute many synapses onto the postsynaptic cell, and so the whole cell postsynaptic recording is only able to provide a measure of P_r that is averaged over all inputs.

In comparison to electrophysiological methods, optical methods are able to provide a much more direct measurement of P_r at individual synapses. Introducing a fluorescent calcium indicator into a postsynaptic neuron allows for the visualization of excitatory postsynaptic calcium transients (EPSCaTs) in individual spines. Measuring the likelihood of producing an EPSCaT in response to low-frequency afferent neuron stimulation provides an approximate measure of P_r at individual synapses (Emptage et al., 1999; Enoki et al., 2009). However, it remains possible that even a single spine receives multiple presynaptic inputs.

Several presynaptic methods of measuring P_r have been explored; these methods allow for the measurement of P_r at individual presynaptic release sites. Styryl dyes, such as FM1-43, allow for the quantification of neurotransmitter release from a presynaptic neuron. Lipophilic fluorescent dye is applied in solution to stain the external neural membrane, and a train of electrical stimuli is applied to induce exocytosis and subsequent endocytosis of all recycling-competent SVs. During endocytosis of the released vesicles, dye is incorporated into the vesicular membrane, where it remains after the dye is washed from the cell surface. Vesicular release is then visualized as a decrease in synaptic fluorescence. Measuring the decrease in fluorescence in response to a single stimulus applied to the presynaptic neuron provides a measurement of P_r (Murthy et al., 1997). One limitation of this method is that incorporation of dye into the vesicular membrane is dependent on the degree of endocytosis, making it difficult to assess exocytosis

independently of the factors that regulate vesicle recycling. It is also difficult to assess short-term changes in release probability because with each re-application of styryl dye, more dye becomes incorporated into the synaptic membrane and adds to the measurement noise (Gaffield and Betz, 2007; Kavalali and Jorgensen, 2014).

P_r has also been measured presynaptically through the use of the genetically encoded pH-sensitive fluorophore, pHluorin (Miesenböck et al., 1998). When tagged to a protein embedded in the vesicular membrane, pHluorin fluorescence is quenched by the acidic environment of the synaptic vesicle lumen. As a vesicle is exocytosed, the pHluorin chromophore becomes deprotonated by the elevated pH of the extracellular milieu and undergoes an increase in fluorescence. Quantifying the change in fluorescence at a synaptic terminal in response to a single action potential provides a direct measurement of P_r at individual release sites (Matz et al., 2010; Zhao et al., 2011, Hoppa et al., 2012).

1.2 PLASTICITY

1.2.1 Hebbian Plasticity

Synapses undergo activity-dependent changes in strength, whereby the strength of a synapse increases following coincident activity of the presynaptic and postsynaptic neurons (Bliss and Lømo, 1973; Bliss and Collingridge, 1993). This form of plasticity is often termed Hebbian plasticity in reference to its identification and characterization by Donald Hebb in 1949. The application of a brief, high-frequency train of stimuli to the excitatory pathways of the hippocampus results in an increase in synaptic strength that lasts between 30 minutes and several hours, depending on the preparation that is used

(Bliss and Lomo, 1973; Bliss and Collingridge, 1993). Enhanced synaptic efficacy on this timescale is referred to as long-term potentiation (LTP) and is most commonly studied in the hippocampus, where it is believed to form the biological basis for the processes of learning and memory. The functional inverse to LTP is long-term depression (LTD), which is typically induced via low-frequency electrical stimulation (Stevens and Wang, 1994; Montgomery and Madison, 2002).

At many synapses, the type of plasticity elicited depends on the precise timing between the activation of the presynaptic and postsynaptic neurons during a stimulus train. At Schaffer collateral synapses, LTP will be initiated if the presynaptic neuron is repeatedly depolarized less than 25 msec before the postsynaptic neuron, whereas LTD will be expressed if the order of firing is reversed (Debanne et al., 1994; Bi and Poo, 1998). LTP has been most intensely studied at two types of synapses, the Schaffer collateral and mossy fibre synapses of the hippocampus, which show marked differences in regard to the induction and expression of long-term plasticity.

Schaffer Collateral LTP

At Schaffer collateral synapses onto CA1 pyramidal neurons in the hippocampus, LTP is induced by postsynaptic mechanisms. Evidence for this comes from the observation that LTP induction in this population is dependent on NMDAR activation (Collingridge et al., 1983). Since NMDAR activation is voltage-dependent, depolarization of the postsynaptic membrane is required to generate LTP, and it must happen within milliseconds of the activation of the presynaptic cell (Wigstrom et al., 1986). Once activated, NMDARs are permeable to calcium (Nowak et al., 1984; Ascher

and Nowak, 1988). The induction of LTP is blocked by injecting a calcium chelator into the postsynaptic neuron (Lynch et al., 1983; Bliss and Collingridge, 1993), supporting the idea that a rise in postsynaptic calcium concentration is required to induce sustainable changes in synaptic strength.

Despite the fact that NMDAR activation is required to induce LTP at Schaffer collateral synapses, there is no change in the number of NMDARs on the postsynaptic membrane following LTP induction (Carroll et al., 1999, but see Grosshans et al., 2002). In contrast, there is a clear increase in the number of AMPARs (Carroll et al., 1999; Pickard et al., 2001) at the synapse within 15-30 minutes of LTP induction (Malinow and Malenka, 2002). The increase in AMPAR number is prevented by an NMDAR blockade (Lissin et al., 1998; Shi et al., 1999).

Some groups have reported that there are no presynaptic changes following LTP induction at Schaffer collateral synapses (Zalutsky and Nicoll, 1990). However, there is recent evidence to suggest otherwise. The application of high-frequency stimulus trains to induce LTP in hippocampal neurons leads to an increase in P_r (Emptage et al., 2003). Silent synapses do not experience an increase in P_r following the same protocol, but are converted from silent to active synapses. After this conversion, a second LTP-induction protocol increases the P_r of the synapse (Ward et al., 2006). Whether Schaffer collateral LTP is regulated primarily by presynaptic mechanisms, postsynaptic mechanisms, or a combination of both, is a question that has not yet been completely resolved.

Mossy Fibre LTP

In contrast to Schaffer Collateral synapses, NMDAR activation is not required to produce LTP at mossy fibre synapses onto CA3 pyramidal neurons (Harris and Cotman, 1986). Long-term plasticity at these synapses is expressed presynaptically (Nicoll and Malenka, 1995) as increase in P_r following LTP induction (Zalutsky and Nicoll, 1990; Weisskopf and Nicoll, 1995; Granger and Nicoll, 2013). There is an increase in glutamate concentration in the mossy fibre synaptic cleft for several hours following LTP induction (Dolphin et al., 1982; Bliss and Collingridge, 1993) which may be the result of an increase in the release probability of a single vesicle, but it may also reflect an increased likelihood of multivesicular release (Reid et al., 2004; Bender et al., 2009). In addition, it appears that presynaptic calcium currents are crucial for the induction of mossy fiber LTP. A reduction of the extracellular calcium concentration completely eliminates LTP induction in this population (Ito and Sugiyama, 1991). Some groups have produced evidence for an involvement of postsynaptic calcium signalling in mossy fiber LTP (Yeckel et al., 1999), but this notion has been questioned (Mellor and Nicoll, 2001).

1.2.2 Homeostatic Plasticity

Unlike Hebbian plasticity, which modulates the efficacy of individual synapses, homeostatic plasticity involves a global scaling of synaptic strength at all synapses of a postsynaptic neuron (Lazarevic et al., 2013; Davis et al., 2013). Due to the fact that it is most frequently induced through changes in network activity, homeostatic scaling has been proposed to act as a compensatory mechanism which stabilizes activity by maintaining synaptic firing rates within an optimal range while preserving the relative differences in efficacy between synapses (Turrigiano et al., 1998; Davis et al., 2013).

There is abundant evidence for an increase in postsynaptically expressed AMPARs following chronic network activity suppression (O'Brien et al., 1998; Wierenga et al., 2005; Thiagarajan et al., 2005; Ibata et al., 2008; Hou et al., 2008). Postsynaptic calcium currents have also been implicated to play a role in homeostatic plasticity; the expression of NMDARs with reduced calcium permeability prevents the induction of homeostatic plasticity (Pawlak et al., 2005), as does blocking the function of dendritic L-type calcium channels (Goold and Nicoll, 2010).

Presynaptic contribution to homeostatic plasticity

Whether homeostatic scaling of synaptic strength has presynaptic expression components or can be attributed entirely to postsynaptic expression mechanisms is somewhat controversial. Some groups report a change in P_r in response to pharmacological manipulations of neuronal activity (Murthy et al., 2001; Thiagarajan et al, 2005; Zhao et al., 2011), whereas others detect no presynaptic change (Goold and Nicoll, 2010; Wierenga et al., 2005, but see Wierenga 2006). It is currently unclear how the use of different electrophysiological and optical techniques to assess presynaptic function in these studies, as well as the differences in preparations used, have contributed to the diversity of the findings. Furthermore, among studies that support homeostatic changes in P_r, there is disagreement as to the mechanism that regulates these changes. For example, one study employing styryl dyes to assess SV exocytosis in dissociated hippocampal neurons following neuronal silencing with TTX reports an increase in RRP size following homeostatic plasticity that corresponds to an increase in P_r (Murthy et al., 2001), whereas the results of more recent work addressing the mechanism of homeostatic

plasticity in the same preparation using a genetically encoded sensor of vesicle exocytosis (Zhao et al., 2011) reported RRP size to be unchanged following homeostatic plasticity. Instead, the authors reported compensatory changes in presynaptic calcium current (Zhao et al., 2011), which implicates the involvement of voltage-gated calcium channels in the expression of homeostatic plasticity. Supporting this notion, increases in the synaptic expression of P/Q-type calcium channels and RIM, a scaffolding protein known to recruit calcium channels to the active zone cytomatrix, have been observed following neuronal activity depletion (Lazarevic et al., 2011). In summary, it is currently unknown whether homeostatic changes in synaptic strength are accompanied by changes in release probability and, if so, whether this altered P_r results from a modulation in RRP size or a change in calcium flux.

1.2.3 Short-term Plasticity

Not all changes in synaptic strength persist for hours or days; short-term plasticity (STP) on the timescale of milliseconds to minutes is also possible. Post-tetanic potentiation is an increase in synaptic strength that is expressed as an increase in P_r following a long, high-frequency stimulus train. It has a decay time constant between tens of seconds and several minutes, depending on the length of the induction stimulus (Bao et al., 1997). Augmentation is an enhancement of synaptic strength with a smaller decay time constant. Following induction by a stimulus train of moderate frequency and length, augmentation fades within several seconds (Zengel and Magleby, 1982; Kamiya and Zucker, 1994). Even a single previous action potential can lead to the facilitation of synaptic transmission, but this paired-pulse facilitation decays quickly, over the time

course of several hundred milliseconds. Short-term depression is a transient reduction synaptic strength that can occur in response to a single prior stimulus and persist for several seconds after being induced.

Short-term facilitation and short-term depression can be quantified by determining the paired-pulse ratio (PPR). To obtain a PPR measurement, two stimuli with a very short interpulse interval are applied to a presynaptic afferent. The amplitudes of the changes in postsynaptic membrane potential are measured with whole-cell recording and are compared between the first and second pulse (Stevens and Wang, 1995). Facilitation is indicated by an increase in amplitude between the first and second stimuli, resulting in a PPR value greater than 1; a PPR value less than 1 indicates the presence of short-term depression. A wide range of interpulse intervals have been used to measure PPR, from 20 msec to hundreds of msec. Shorter interpulse intervals are associated with a larger magnitude of facilitation (Mennerick and Zorumski, 1995; Atluri and Regehr, 1996; Salin and Nicoll, 1996).

Short-term plasticity is believed to serve as an information filtering mechanism that regulates the peak responsiveness of a neuron in the face of inputs of different frequencies (Fortune and Rose, 2001; Abbott and Regehr, 2004). For example, depressing synapses transmit information optimally at low firing frequencies or at the onset of input, whereas facilitating synapses transmit information optimally during sustained, high-frequency firing (Fuhrmann et al., 2002; Abbott and Regehr, 2004). Changes in short-term facilitation and depression therefore have the potential to influence synaptic integration in the postsynaptic neuron and may lead to alterations in the

frequency of spike output and subsequent transmission of information.

Mechanisms of short-term facilitation

Facilitation is common at synapses with an initially low P_r , such as hippocampal mossy fiber synapses. Calcium buffering with high concentrations of EGTA reduces the amount of synaptic enhancement that occurs in response to trains of stimuli at mossy fiber synapses (Regehr et al., 1994), raising the possibility that short-term facilitation is induced by presynaptic calcium.

The "residual calcium hypothesis" of facilitation states that calcium remaining in the terminal from a prior action potential leads to an increase in the probability of release during a subsequent action potential (Wu and Saggau, 1994; Kamiya et al., 2002). Residual calcium facilitates release through several mechanisms, including modulation of the pool of docked vesicles, regulation of vesicle priming, modulation of calcium influx through voltage-gated calcium channels, or saturation of calcium buffers, leading to larger action potential-evoked calcium transients (Fioravante and Regehr, 2011).

Enhancement of the presynaptic calcium current results in faster replenishment of the RRP following release (Wang and Kaczmarek, 1998; Dittman and Regehr, 1998; Hosoi et al., 2007), which may be explained by an increase in the rate of vesicle priming. Short-term plasticity varies depending on which isoform of the vesicle priming protein Munc-13 is present at the synapse (Rosenmund et al., 2002, Junge et al., 2004). Enhanced calcium current may also regulate short-term plasticity by modifying calcium channel conductance through the action of calcium-sensor proteins (Mochida et al., 2008; Leal et al., 2012), as outlined above.

The coupling of vesicles to calcium channels may additionally play a role in short-term facilitation. There is evidence that each RRP is made up of vesicles of heterogenous vesicular release probabilities (vP_r; Meinrenken et al., 2002; Scimemi and Diamond, 2012). Vesicles that are closely coupled to calcium channels are more likely than loosely-coupled vesicles to be triggered for exocytosis in response to a calcium current. For vesicles that are far away from calcium channels, and have low vP_r, calcium build-up in the terminal may be necessary to trigger release because the calcium must diffuse farther throughout the terminal before it can reach the vesicle and trigger exocytosis. When stimuli are delivered in close succession, calcium that remains in the presynaptic terminal after an action potential may partially saturate calcium buffering proteins. Calcium entering the terminal in response to the next stimulus is then able to diffuse further and trigger the release of synaptic vesicles that are a greater distance from the open calcium channel (Felmy et al., 2003; Eggermann et al., 2012). In this way, calcium remaining in the terminal effectively increases the number of vesicles available for exocytosis, which briefly raises the release probability of the synapse and results in paired-pulse facilitation.

Mechanisms of short-term depression

The readily-releasable pool of docked and primed SVs at synapses in the central nervous system is generally quite small. On average, cultured rodent hippocampal synapses have several hundred vesicles in the reserve pool, approximately 10 of these vesicles are docked at the active zone (Schikorski and Stevens, 1997) and only a subset of the docked pool is available for release as part of the RRP. Since the size of the RRP is

limited, whenever a proportion of the pool is depleted in response to a stimulus, P_r will be temporarily reduced until the RRP is replenished with vesicles from the recycling pool. This is the RRP depletion model of short-term depression (Betz, 1970; Stevens and Wang, 1995).

The RRP depletion model is supported by demonstrations that the extent of the reduction in P_r during STP correlates with the magnitude of RRP depletion at that synapse (Kusano and Landau, 1975). To assess the relationship between RRP depletion and synaptic depression, several studies have utilized techniques that elicit the exocytosis of synaptic vesicles by means other than the action potential-evoked opening of voltage-gated calcium channels, such as the extracellular application of a hypertonic solution (Rosenmund and Stevens, 1996) or the flash photolysis of caged calcium (Schneggenburger et al., 1999). These techniques elicit a depression of synaptic transmission that is very similar in its degree and recovery time course to the depression elicited by electrical stimulation. Additionally, the depression initiated by these techniques occludes the depression initiated by electrical stimulation, indicating that they act through the same mechanism. Together, this evidence suggests that synaptic depression is mainly a consequence of the depletion of the RRP.

In addition to RRP depletion, other mechanisms that may contribute to synaptic depression include autoinhibition by neurotransmitter acting on presynaptic metabotropic receptors (Davis et al., 1993), inactivation of presynaptic calcium channels (Patil et al., 1998; Xu and Wu, 2005), reduced calcium sensitivity of the presynaptic release machinery (Hsu et al.,1996; Waldeck et al., 2000), failure of action potential propagation (Smith and Hatt, 1976) or changes in action potential waveform which lead to a reduction

in calcium influx and subsequently reduce neurotransmitter release (Brody and Yue, 2000). Postsynaptic mechanisms such as receptor desensitization (Trussel and Fischbach, 1989) or saturation (Sun and Beierlein, 2011) may also contribute to short-term synaptic depression.

Although depression is the dominant form of STP at some synapses, and facilitation is dominant at others, they may both occur in the same populations and even within the same synapses (Dittman et al., 2000; Muller et al., 2010). It therefore seems that RRP depletion and residual calcium occur in combination to produce either net depression or net facilitation at a particular synapse.

Relationship between P_r and PPR

From the preceding discussion of mechanisms that modulate P_r and PPR, it is clear that these two synaptic properties may be closely associated. This notion is supported by several lines of experimental evidence. First of all, populations of synapses with an initially high P_r are commonly observed to undergo PPD, and populations with initially low P_r are likely to undergo PPF (Debanne et al., 1996; Silver et al., 1998). Additionally, the manipulation of extracellular calcium concentration or presynaptic calcium buffering modulates P_r and PPR inversely (Dittman and Regehr, 1998; Kravchenko et al., 2006). Inverse changes of P_r and PPR have been witnessed during long-term potentiation of hippocampal mossy fibre synapses (Zalutsky and Nicoll, 1990) and potentially also Schaffer collateral synapses (Emptage et al., 2006, but see Zalutsky and Nicoll, 1990). Finally, some pharmacological manipulations that increase P_r, such as

the application of forskolin to increase glutamate release, also increase PPD (Bender et al., 2009).

While some experimental manipulations inversely affect P_r and PPR, it remains unclear whether all mechanisms that modulate release probability also influence paired-pulse plasticity. The use of electrophysiological methods to address this question is limited. As previously discussed, whole cell recording provides an indirect measure of P_r, and techniques such as NMDA receptor blockade by MK-801 critically rely on a number of assumptions that are difficult to verify. Moreover, electrophysiological experiments typically measure an aggregate response from a pool of synapses that likely contains synapses expressing diverse release probabilities and paired-pulse plasticities.

In contrast to electrophysiological techniques, optical methods allow for the direct quantification of release probability at individual synapses. Although genetically encoded indicators of synaptic vesicle exocytosis such as synaptophysin-pHluorin have not yet been used to assess paired-pulse plasticity, they should be adaptable to this purpose and therefore appropriate to determine the relationship between P_r and PPR at the level of individual synapses.

As previously discussed, the release probability of synapses can be modulated through two sets of mechanisms. The first set includes processes which alter the number of readily releasable synaptic vesicles at the synapse (RRP size); the second set encompasses mechanisms which modulate the likelihood that an individual SV in the readily releasable pool will undergo exocytosis (vesicular release probability, vP_r). Previous evidence suggests that mechanisms which alter vP_r, such as changes in presynaptic calcium flux or in the spatial coupling between calcium channels and docked

vesicles, also affect paired-pulse plasticity, leading to inverse changes of P_r and PPR. However, it remains unclear whether PPR is also influenced by processes regulating the size of the RRP. We hypothesize that modifications in the size of the RRP lead to changes in P_r without affecting paired-pulse plasticity. An experimental validation of this hypothesis would be significant in two respects. First, it would demonstrate that synaptic reliability and short-term plasticity can be independently altered at individual synapses. A mechanism that alters P_r of a synapse without changing PPR would add to the computational power of a synapse because it would allow for changes in synaptic strength without altering the "frequency tuning" of the synapse, i.e. its ability to transmit information best at certain presynaptic firing frequencies. Secondly, our findings would indicate that the absence of changes in paired-pulse ratio should not be taken as evidence for unaltered release probability, as it is currently done in many electrophysiological studies.

CHAPTER 2: MATERIALS AND METHODS

2.1 GENERAL PROTOCOLS

2.1.1 Primary Cultures of Hippocampal Neurons

All experiments were conducted in dissociated cultures of rat embryonic hippocampal neurons. Sprague-Dawley rat embryos were dissected at E18. Hippocampi were incubated with 0.03% trypsin for 15 minutes and then dissociated using a pasteur pipette. Neurobasal medium (Invitrogen) was supplemented with 1% B27, 0.5 mM glutamine, and 0.5 μM glutamate. Cells were diluted in 5% fetal calf serum and plated with a density of $3x10^3/cm^2$ onto 12 mm glass coverslips. Cells were stored in an incubator at 5% CO_2 and 37°C, with five coverslips per 60 mm culture dish. Twenty-four hours after the cells were plated, the supplemented medium was replaced with serum-free Neurobasal media containing 1% B27.

2.1.2 Calcium Phosphate Transfections

Calcium phosphate transfections were used to introduce cDNA constructs into hippocampal cultures 11-14 days after the cells were plated. At this stage, the neurons are mature enough to have formed functional synapses (Basarsky et al., 1994), but still young enough to effectively take up foreign DNA during transfection.

The medium in each culture dish to be transfected was replaced with MEM (Invitrogen) containing 1% B27. The original medium was filtered through a 0.22 μm sterile filter and kept for later use. A precipitation mix was prepared for each culture dish, consisting of 20-80 μg of every DNA construct to be expressed, 0.25 M $CaCl_2$, and enough water to bring the total volume to 300 μL. Precipitation mixes for all experiments contained a fluorescent reporter for synaptic vesicle exocytosis, synaptophysin-pHluorin

(sypHl). Each sypHl construct contained either two or three pHluorin proteins; no differences were observed in expression level or sensitivity between constructs, and so no distinction was made between them during analysis. Each mix was added in 30 μL increments to 300 μL of HEBS buffer (274 mM NaCl, 10 mM KCl, 1.4 mM Na_2HPO_4, 15 mM D-glucose, 42 mM (2-hydroxyethyl)-1-piperazineethanesulfonic acid (Hepes), pH 7.10) and left to sit at room temperature for 20 minutes to allow calcium phosphate precipitate to form. Mixes were then pipetted dropwise onto coverslips, and cultures were incubated at 5% CO_2 and 37°C for 4-16 hours before being rinsed with a wash buffer (144 mM NaCl, 3 mM KCl, 2 mM $MgCl_2$, 10 mM Hepes, pH 6.70) to remove precipitate. Following the wash, the original medium in which the cultures were maintained was returned and the cells were incubated at 5% CO_2 and 37°C. Approximately 2-10% of neurons in each dish could be transfected using this method, depending on the size of the transfected plasmid and its protein product. Expression of the target protein coded by the transfected DNA peaked 2-4 days following transfection.

2.1.3 Fluorescence Imaging

Prior to imaging, glass coverslips were removed from the culture dish and placed in a stimulation chamber with platinum electrodes. Coverslips were submerged in HBS solution (124 mM NaCl, 3 mM KCl, 2 mM $CaCl_2$, 1 mM $MgCl_2$, 10 mM Hepes, and 5 mM D-glucose, adjusted to pH 7.30 and 270 mOsm). The HBS solution was supplemented with 10 μM DNQX and 50 μM APV to prevent recurrent synaptic activity by blocking AMPA and NMDA receptors, respectively. The stimulation chamber was

then placed on a heated (37°C) microscope stage of a Nikon TE2000 inverted fluorescence microscope equipped with a 60x oil immersion objective, a Spectre X LED light source (Lumencor, Beaverton OR), and a Sutter lambda 10.2 emission filter (Sutter Instruments).

For sypHl visualization, a 475/28 nm LED light source, dichroic with 500-800 nm transmission band, and 525/50 emission filter were used (Semrock, Rochester, NY). For mCherry-containing constructs, a 575/25 nm LED light, dichroic with 601-800 nm transmission band and 624/40 nm emission filter were used. All images were acquired with a Hamamatsu ORCA CCD camera and the acquisition was controlled by custom scripts written and executed using IPlab software.

2.1.4 Stimulus Protocols

To identify neurons that were transfected with sypHl, fields were stimulated with a 2 sec, 20 Hz stimulus train. Following synaptic vesicle exocytosis triggered by field depolarization, the pHluorin molecule experiences an increase in environmental pH and undergoes deprotonation of its chromophore, which leads to an increase in fluorescence (ΔF). When a transfected axon was optically identified by a change in fluorescence, it was centered in the field of view and a phase image was acquired before the experiment was conducted.

Release probability was investigated by applying a 1 ms square bipolar current (10 V/cm) to the field in order to elicit a single action potential (Zhao et al., 2011). Fluorescent responses were recorded for 600 msec at a rate of 10 frames per second (fps), with the stimulus being delivered immediately following the third frame (**Fig 1**).

Acquisition rate was limited by the frame rate and photon sensitivity of the camera. ΔF(1AP) is proportional to P_r so long as sypHl expression level is consistent between synapses, as it is between the synapses of a single presynaptic axon, or between neurons with comparable basal fluorescence levels.

To obtain a measurement of paired-pulse ratio at synapses, a pair of stimuli separated by 25 msec were applied to the field. The temporal resolution of our imaging system was not sufficient to resolve fluorescence increases in response to individual stimuli spaced 25 msec apart. However, we reasoned that the change in sypHl fluorescence in response to two stimuli corresponds to the sum of the individual responses. This assumption relies on previous findings that sypHl fluorescence decay following release and subsequent endocytosis is generally slow (tau_{slow}=20s, tau_{fast}=2s, Granseth et al., 2006) in comparison to our stimulation and acquisition paradigm.

At a given synapse, ΔF scales proportionally with the number of vesicles that are released. The size of the RRP was estimated by delivering an intense (80AP, 40 Hz) stimulus train to trigger the release of all docked and primed vesicles at each synapse. Images were acquired over 2 seconds at a rate of 10 fps, with the stimulus being applied immediately following the third frame.

ΔF(1AP) and ΔF(2AP) were measured with a single acquisition script, in the following pattern: (1AP) x2, (2AP) x1 repeated 5 times with 5 second intervals between trials to allow for vesicle reacidification and fluorescence quenching. Following this sequence of stimuli, the RRP-depleting stimulus train was delivered. This procedure was repeated between 8-10 times to produce between 80-120 total trials for ΔF(1AP), 40-60 trials for ΔF(2AP) and 8-12 trials for ΔF(80AP, 40Hz). A single experiment was defined

as the completion of the full stimulation protocol, and measurement of the resulting fluorescent responses at the synapses of a single axon on the coverslip. Experiments were excluded if a comparison between initial and final RRP ΔFs revealed a significant (>30%) reduction in responsiveness over the course of the experiment.

2.1.5 Image Analysis

Images were analyzed using custom scripts in IPlab and IgorPro. Images were first aligned to correct for small field shifts during acquisition, and then background-subtracted using a rolling ball algorithm. Synapses were identified optically at regions along the axon experiencing an increase in fluorescence. In initial experiments, these areas were manually selected as regions of interest (ROI) using an image generated by averaging the responses to single and pairs of stimuli as a template. All manually selected ROIs were 1.44 μm^2. In later experiments (homeostatic plasticity, mSYD1A knockdown and overexpression), we used an automated threshold and size-constraint based method of ROI selection similar to that described by Bergsman et al. (2006) and implemented in IPLab, which resulted in smaller ROIs between 0.64-1.0 μm^2. Synapses were excluded when the responses of adjacent synapses to the 2s, 40 Hz stimulation were not clearly separated. Experiments were excluded if fewer than six synapses could be identified along a single transfected axon.

Fluorescence intensity changes at selected regions of interest were averaged over all trials for each experiment. In the single-stimulus condition, baseline fluorescence (frames 2 and 3, prior to stimulation) was subtracted from the average fluorescence of frames 4-5 at each synapse to obtain the average fluorescent change in response to one stimulus [ΔF(1AP)], an indirect measure of release probability (Matz et al., 2010).

To calculate PPR, the average fluorescence change in response to a paired, 40 Hz stimulation [ΔF(2AP)] for each synapse was measured by subtracting the baseline fluorescence (frames 2 and 3, prior to stimulation) from the average fluorescence values over frames 4-5. The size of the response to the second stimulus in the pair can be estimated by subtracting the average ΔF(1AP) from the average ΔF(2AP) for each synapse. PPR can then be calculated according to the following:

$$\text{PPR} = \frac{\Delta F(2(AP) - \Delta F(1AP)}{\Delta F(1AP)}$$

The size of the RRP was measured by taking the average difference in fluorescence intensity prior to stimulation (frames 1-3) and the peak fluorescence value (frames 25-27).

2.2 MODIFICATION OF EXTRACELLULAR CALCIUM CONCENTRATION

2.2.1 Alternating Calcium Buffers

Dissociated cultures of hippocampal neurons were transfected with sypHl using the previously-described calcium phosphate transfection protocol. Cells were incubated for 3 days before imaging. Throughout the experiment, the standard HBS buffer used for imaging (2 mM $CaCl_2$) was alternated with HBS buffer containing 4 mM $CaCl_2$. Buffers were exchanged without removing the coverslip from the stage by using a slow perfusion system (Warner Instruments) and a peristaltic suction pump (Reglo Ismatec).

Four rounds of the stimulus protocol (consisting of a single, pair, and train of stimuli) were conducted in 2 mM $CaCl_2$ before the buffer was replaced with 4 mM $CaCl_2$ for eight rounds, then replaced once more with 2 mM $CaCl_2$ for a final four rounds. In total, four experiments were completed (n=4 axons, each from different a neuron culture).

The ΔF(1AP) and PPR values were compared between 2mM and 4mM calcium conditions using a nonparametric Wilcoxon matched-pairs signed-ranks test. Nonparametric tests were selected due to the non-normal distribution of probabilities that was confirmed with a Shapiro-Wilk test.

2.3 CHRONIC ACTIVITY SUPPRESSION IN VITRO

2.3.1. TTX Application

Neuron cultures were transfected with sypHl according to the calcium phosphate transfection protocol outlined above. Immediately following transfection, the medium in half of the culture dishes was supplemented with 5 μM TTX to suppress neural activity via blocking of Na^+ channels. Culture dishes from TTX-positive and TTX-negative groups were incubated at 37°C and 5% CO_2 for 48 hours.

Immediately before imaging, coverslips that were removed from dishes containing TTX were rinsed with a washing buffer (144 mM NaCl, 3 mM KCl, 2 mM MgCl2, 10 mM Hepes, pH 6.70) for 2-3 minutes to remove all traces of the drug. The experiment was conducted according to the previously described imaging protocol.

The median ΔF(1AP), ΔF(2AP) and ΔF(80AP, 40Hz) values from each experiment were compared between TTX-positive and TTX-negative groups with unpaired t-tests. Each experiment consisted of a single axon from one coverslip; one TTX-positive coverslip and one control coverslip were taken from each of six different neuron cultures (n_{TTX}=6 axons, n_{CTRL}=6 axons).

2.4 SYD1A KNOCKDOWN

2.4.1. Testing a SYD1A Knockdown Construct

An shRNA construct against the target sequence ctggtgagatttggtacaa in rat SYD1A (nt 320-338, numbering relative to start codon in reference sequence with Geneback accession number XM_343173) was generated by synthesizing oligonucleotides (5'-ccgg-ctggtgagatttggtacaa-ctcgag-ttgtaccaaatctcaccag-tttttc-3' and 5'-aattcaaaaa-ctggtgagatttggtacaa-ctcgag-ttgtaccaaatctcaccag-3'). The oligonucleotides were phosphorylated, annealed, and ligated into AgeI and EcoRI-cut pSs_u6, an shRNA expression vector derived from pSuper.basic (Oligoengine). To test the efficiency of this construct, cell cultures were transfected with a cytosolic-BFP and an EGFP-tagged SYD1A construct using the calcium phosphate transfection protocol. Half of the cultures were also transfected with the mSYD1A-targeting shRNA construct, and the rest were transfected with a pSs_u6 vector lacking the shRNA sequence to serve as a control.

Baseline EGFP fluorescence was assessed 2-3 days following the transfection using a 470/22 nm excitation filter, R:400-490/T:500-800 dichroic, and a 525/50 nm emission filter. BFP fluorescence was measured using a 387/11 nm excitation filter, R:344-404/T:415-570 dichroic, and a 447/60 nm emission filter. The images were then analyzed using IPLab. Regions of interest were manually selected along the visibly transfected axons in each field, each spanning the entire width of the axon on which it was drawn. Six regions were selected from a minimum of two different axons in each field. The ratio of EGFP:BFP fluorescence was compared between groups to determine knockdown efficiency between knockdown and control cultures.

2.4.2 Assessing Neurotransmitter Release in Cultures with Reduced SYD1A Expression

All cultures were transfected with sypHl. Half of the cultures were transfected with SYD1A knockdown construct, and the rest were transfected with the pSS_u6 construct lacking a knockdown construct to act as a control. Prior to imaging, the experimenter was blinded by the replacement of the identifying labels on the culture dishes with generic group labels. Cells were imaged as described previously to measure ΔF(1AP), ΔF(2AP) and ΔF(80AP, 40Hz) at each synapse. Each experiment consisted of a single axon from one coverslip; two SYD1A-KD expressing coverslips and two control coverslips were taken from each of three different neuron cultures (n_{KD}=6 axons, n_{CTRL}=6 axons).

2.5 SYD1A OVEREXPRESSION

The cDNA for rat SYD1A was cloned via RT-PCR. The clone used was identical to Genebank reference sequence XM_343173 except for point mutations a922g (aa substitution S308G), c1166t (A389V) and a2068g (S690G), which occurred in three independent clones analyzed from the RT-PCR and most likely represent strain differences. The SYD1A n-terminus was tagged with mCherry and inserted into an expression plasmid containing a CMV promoter.

Cultures were transfected with sypHl, and either SYD1A tagged with mCherry or mCherry alone, according to the calcium-phosphate transfection protocol. The experimenter was blinded prior to the experiment by removing labels from the culture dishes. During imaging, transfected cells were identified by the presence of mCherry fluorescence and the experiment was conducted as described previously to obtain

measurements of ΔF(1AP), ΔF(2AP) and ΔF(80AP, 40Hz). Each experiment consisted of a single axon from one coverslip; two SYD1A overexpressing coverslips and two control coverslips were taken from each of five different neuron cultures (n_{SYD}=10 axons, n_{CTRL}=10 axons).

CHAPTER 3: RESULTS

3.1 PAIRED-PULSE RATIO IS HIGHLY VARIABLE BETWEEN SYNAPSES OF A SINGLE PRESYNAPTIC NEURON

In cultured hippocampal neurons transfected with sypHl, a genetically encoded sensor of synaptic vesicle exocytosis, release probability at individual synapses can be assessed by quantifying the average increase in fluorescence in response to an isolated action potential (**Fig. 1**). This technique has been utilized in previous work to investigate the relationship between active zone size and release probability at individual synapses between hippocampal neurons in culture (Matz et al., 2010). However, it has not yet been used to assess short-term plasticity at individual presynaptic release sites. In electrophysiological experiments, paired-pulse plasticity is measured by quantifying the paired-pulse ratio, i.e. the ratio of EPSC amplitudes evoked by two successive stimuli (**Fig. 1E**). In experiments with sypHl, the temporal resolution of imaging acquisition was not sufficient to resolve fluorescence increases in response to two individual stimuli at high frequency. However, on the assumption that the change in sypHl fluorescence in response to two consecutive stimuli delivered in short succession is equal to the sum of the fluorescence increases for each stimulus, the paired-pulse ratio of synaptic vesicle exocytosis (PPR_E) can be calculated from aggregate responses to paired stimuli, $\Delta F2$, and responses to isolated stimuli, $\Delta F1$, as $PPR_E = (\Delta F2 - \Delta F1)/\Delta F1$ (**Fig. 1F**). Our assumption relies on the previous finding that the endocytosis and re-acidification of SVs is relatively slow (Sankaranarayanan and Ryan, 2000; Granseth et al., 2006) and thus negligible over the timespan of the acquisition of fluorescence changes in response to paired stimuli. It should be noted that values of PPR_E can conceivably differ from electrophysiologically obtained paired-pulse ratios, as the latter are influenced by postsynaptic modulation

(receptor desensitization and saturation) in addition to the short-term plasticity of release. In initial experiments, we addressed whether paired-pulse plasticity at individual synapses can be reliably assessed with sypHl (**Fig. 2**). We found that increases in sypHl fluorescence following a single action potential (1AP) or a pair of action potentials (2AP) were clearly discernible (**Fig. 2A-B**). The average PPR_E of all synapses along a single axon was 2.08 (n = 4 axons, 99 synapses; interpulse interval 40 msec). Our results are very similar to PPR values obtained electrophysiologically at Schaffer collateral synapses (Stevens and Wang, 1995; Salin et al., 1996; Dittman et al., 2000), and to the average PPR at synapses between hippocampal neurons in dissociated culture determined using styryl dyes (Murthy et al., 1997). PPR_E values of individual synapses varied strongly around this average; the standard deviation of PPR_E values in a population of 99 synapses from four axons was 2.42. There is some evidence that this variance may be attributed to the presence of different neuronal cell types in culture, which are likely to display differences in their short-term plasticity (see, e.g. Salin et al., 1996; Dittman et al., 2000). Due to the sparse transfections of our neuronal cultures, we were often able to visually identify individual axons and compare synapses along single identified axons. Interestingly, we found that the variability of PPR_E among the synapses along an individual axon was comparable to the variability of PPR_E values of all synapses (**Fig. 2E**). The large variability observed within each axon supports the notion that paired-pulse plasticity may be regulated at the level of individual synapses.

3.2 RELEASE PROBABILITY AND PPR ARE INVERSELY CORRELATED AT INDIVUAL SYNAPSES

At many synapses, manipulations increasing release probability lead to a decrease in the paired-pulse ratio and vice versa (Debanne et al., 1996; Silver et al., 1998; Pan et al., 2004). This has been interpreted to mean that these properties are interdependent and regulated by the same set of mechanisms. However, this notion has never been thoroughly tested. In a first approach, we therefore asked whether release probability and paired-pulse ratio are also inversely correlated at individual synapses. Among the synapses along a single, visually identified axon, we saw an inverse correlation between release probability and PPR_E (**Fig. 3A1**, Spearman's $r = -0.478$, $p<0.01$). This was true for all axons that were analyzed (**Fig. 3A2**, $r_{av}=-0.458\pm0.035$, n=6 axons, error reported as SEM). However, the inverse correlations were relatively moderate. This finding may indicate that short term plasticity and P_r are regulated by overlapping, but non-identical sets of mechanisms.

3.3 VESICULAR RELEASE PROBABILITY, BUT NOT THE SIZE OF THE RRP, AFFECTS PAIRED-PULSE PLASTICITY

There is a lot of evidence to suggest that release probability is partially determined by the number of docked and primed synaptic vesicles in the readily releasable pool (RRP; Schikorski and Stevens, 1997; Dobrunz and Stevens, 1997; Murthy et al., 2001; Matz et al., 2010; Branco et al., 2010; Holderith et al., 2012). If RRP size affects release probability, and there is an interdependence between P_r and paired-pulse plasticity, the number of docked and primed synaptic vesicles might also affect paired-

pulse plasticity. Before investigating this possibility directly, we first sought to confirm that P_r correlates with RRP size.

In our experiments, release probability and RRP size of synapses along a visually identified axon were strongly correlated. **Figure 3B1** shows a representative experiment in which ΔF(1AP) and RRP size showed a positive correlation (Spearman's r=0.683. p<0.0001). There were significant, positive correlations at all axons (**Fig. 3B2**, r_{av}=0.550±0.048, error reported as SEM, n=6 fields), supporting the notion that RRP size is a determinant of P_r. However, despite our findings that release probability is correlated with RRP size, we observed no significant correlation between PPR_E and the size of the RRP among synapses of a visually identified presynaptic axon (**Fig. 3C1**, Spearman's r = 0.090. p=0.574). The average correlation coefficient between PPR_E and RRP (n=6 axons) was 0.175±0.047 (**Fig. 3C2**). This result gives a first indication that short-term plasticity is not influenced by the same mechanisms that regulate RRP size, and that the modulation of RRP size is a potential avenue by which one may alter the release probability of a synapse without changing the PPR.

While release probability is modulated by the size of the readily releasable pool of synaptic vesicles, it also depends on the likelihood that individual synaptic vesicles in the RRP will undergo exocytosis in response to an action potential, the vesicular release probability (vPr; Schneggenburger et al., 2002; Gerber et al., 2008; Scimemi and Diamond, 2012; Ermolyuk et al., 2012). We calculated the average likelihood of release of an individual vesicle ($\overline{vP_r}$) at each synapse by dividing our measure of release probability by the RRP size of the synapse, and investigated the possibility that $\overline{vP_r}$ may co-regulated with PPR. At the synapses of a single axon, we saw a strong negative

correlation between $\overline{vP_r}$ and PPR_E (**Fig. 3D1**, Spearman's r=-0.790, p<0.0001). This was true for all axons that were analyzed (**Fig. 3D2**, r_{av}=-0.661±0.070, n=6 fields). Furthermore, the correlation between $\overline{vP_r}$ and PPR_E was significantly stronger than that between P_r and PPR_E in the same experiments (p<0.01, comparison of Spearman's r-values with a paired t-test, n=6). In summary, our results suggest that the mechanisms regulating vesicular release probability affect both P_r and PPR, whereas mechanisms affecting RRP size may modulate release probability without affecting paired-pulse plasticity.

3.4. PPR STRONGLY CORRELATES WITH THE APPARENTLY CALCIUM SENSITIVITY OF RELEASE

The likelihood with which individual SVs in the readily releasable pool undergo exocytosis in response to an isolated action potential may critically depend on mechanisms regulating local calcium influx at presynaptic release sites (Hoppa et al., 2012) and its spatial coupling with docked and primed synaptic vesicles (Eggermann et al., 2012). Together, these mechanisms determine the apparent calcium sensitivity of neurotransmitter release at a synapse. We sought to determine how the apparent calcium sensitivity of SV exocytosis at individual synapses related to their paired-pulse plasticity. For this purpose, we determined release probabilities and paired-pulse ratios of synapses in both 2 mM and 4 mM calcium-containing buffers (**Fig. 4**). Over all synapses, the increase in fluorescence following a single action potential was significantly higher in 4 mM than in 2 mM calcium (**Fig. 4I**, p<0.001, Wilcoxon matched pairs test), demonstrating that an increase in extracellular calcium raises release probability.

Likewise, PPR_E values were significantly reduced by raising the extracellular calcium concentration (**Fig. 4J**, $p<0.01$, Wilcoxon matched pairs test). This finding is consistent with results of earlier electrophysiological studies showing increases in P_r and a reduced PPR following increases in the extracellular calcium concentration (Rausche et al., 1988; Mennerick and Zorumski, 1995; Dittman and Regehr, 1998; Talpalar and Grossman, 2003; Kravchenko et al., 2006).

Despite the overall increase in P_r and reduction in PPR, individual synapses showed pronounced variability in response to increases in the extracellular calcium concentration. Synapses demonstrating a large increase in ΔF(1AP) following a change in calcium concentration were often facilitating (e.g. **Fig. 4E-F**). Conversely, synapses demonstrating only small changes in ΔF(1AP) following an increase in calcium concentration tended to be depressing (e.g. **Fig. 4G-H**). To compare the calcium sensitivity and PPR of individual synapses in a systematic way, we calculated the ratio of ΔF(1AP) in 4mM calcium to ΔF(1AP) in 2mM calcium. This ratio reflects the fold change in P_r when the extracellular calcium concentration is increased from 2mM to 4mM. The magnitude of the change in P_r following an increase in calcium concentration was strongly correlated with paired-pulse ratio at the individual synapses of a single axon (**Fig. 4K**, Spearman's $r=0.746$, $p<0.001$). This correlation was present along all axons (**Fig. 4L**, n=4 axons). These results suggest that the apparent calcium sensitivity of synapses and their paired-pulse plasticity are closely associated, and implicates mechanisms modulating the apparent calcium sensitivity in the control of paired-pulse plasticity.

3.6 CHRONIC ACTIVITY SUPPRESSION DOES NOT CHANGE THE SIZE OF THE RRP

For the remainder of my thesis work, we aimed to identify mechanisms that regulate the size of the RRP without affecting $\overline{vP_r}$ to provide evidence for an independent modulation of P_r and PPR at individual synapses. Experimental manipulations that suppress neuronal activity have been reported to result in an increase in release probability (Murthy et al 2001; Thiagarajan et al., 2005; Zhao et al., 2011). The results of previous studies addressing the mechanism of homeostatic changes in P_r are somewhat conflicting, however, suggesting either changes in the size of the RRP (Murthy et al., 2001) or alterations in presynaptic calcium influx (Zhao et al., 2011). We reasoned that, if homeostatic plasticity does lead to alterations in RRP size, it may be elicited by mechanisms that change P_r independently of any alterations in paired-pulse plasticity. In support of this idea, it has previously been reported that PPR does not change during homeostatic plasticity, a finding that has been interpreted as evidence for the lack of alterations in P_r (Wierenga et al., 2005; Goold and Nicoll, 2010). To induce homeostatic plasticity, we silenced our cultures with 5 μM TTX for 48 hours following sypHl transfection. We hypothesized that, if homeostatic plasticity resulted in an increase in RRP size without affecting $\overline{vP_r}$, it would be accompanied by an increase in release probability at individual synapses, with no change to PPR.

Release probability, paired-pulse ratio, and RRP size were compared between the synapses of a single TTX-treated axon and those from the axon of a control neuron. These comparisons revealed no significant differences between groups (**Fig. 5A-C**). However, our summary data (n_{TTX}=6, n_{CTRL}=6) revealed a non-significant trend towards

an increase in release probability (**Fig. 5D**, $\Delta F(1AP)_{TTX}$ = 20.5±5.31, $\Delta F(1AP)_{CTRL}$ = 17.6±3.52, p=0.658) and a non-significant decrease in paired-pulse ratio (**Fig. 5E**, PPR_{TTX} = 0.87±0.19, PPR_{CTRL} = 0.92±0.21, p=0.867) following TTX treatment. We briefly considered enlarging this dataset to obtain more conclusive information about if and how release probability may be homeostatically altered, but ultimately decided against it (see discussion). The data we have so far acquired neither confirm nor contradict our hypothesis regarding the influences of RRP size on P_r and paired-pulse plasticity, since silencing with TTX failed to produce any change in the size of the RRP (**FIG. 5F**, p=0.787), and so the question remains as to whether release probability and PPR can be independently modulated through a change in RRP size.

3.7 ALTERING SYD1A EXPRESSION DOES NOT CHANGE THE SIZE OF THE RRP

3.7.1 Neurons expressing a SYD1A knockdown construct show unaltered Pr, PPR and RRP

The number of docked synaptic vesicles, and thus RRP size, may be modulated by the expression of presynaptic proteins. SYD1A is a presynaptic protein that is required for presynaptic differentiation in *C. elegans* (Hallam et al., 2002) and at the *Drosophila melanogaster* neuromuscular junction (Oswald et al., 2010). Recently, it has been demonstrated that the genetic ablation of mSYD1A, one of the two SYD1 homologs in mammals, reduces the number of docked SVs at hippocampal synapses independently of changes in active zone size (Wentzel et al., 2013). Surprisingly, paired-pulse plasticity at CA1 neurons from mice lacking mSYD1A was unaltered. In light of our results regarding the relationship of RRP size, $\overline{vP_r}$ and PPR, these previous findings may indicate that

SYD1A modulates RRP size while leaving $\overline{vP_r}$ unaffected. In an effort to manipulate mSYD1A levels at hippocampal synapses, we performed an shRNA-mediated knockdown of mSYD1A (**Fig. 6A**) in our primary cultures of hippocampal neurons and investigated the effect on release probability and paired-pulse ratio.

A test of the knockdown construct revealed a 54% reduction of mSYD1A in cultures transfected with mSYD1A-KD relative to control cultures (**Fig. 6B**, n_{KD}=36 fields, n_{CTRL}=37 fields). However, in cultures transfected with both mSYD1A-KD and sypHl (n=6 fields), we observed no change in our measure of release probability (**Fig. 7A**, p=0.357, n=6 fields), paired-pulse ratio (**Fig. 7B**, p=0.607), or readily releasable pool (**Fig. 7C**, p=0.357) when compared to controls.

Despite the lack of any significant change in RRP size following the expression of an mSYD1A-KD construct, we did observe a trend towards a reduction in RRP size (RRP_{KD} = 500±83.94, RRP_{CTRL} = 781±137.7). It is possible that with a more severe reduction in mSYD1A expression, or a simultaneous reduction of SYD1A and the homologous protein SYD1B, we may be able to produce a significant change in the size of the RRP.

3.7.2 SYD1A overexpression has no impact on release probability, PPR, or RRP size

Following the SYD1A knockdown experiments, we also attempted to increase the size of the RRP by overexpressing SYD1A-mCherry so that we could investigate the result of modified RRP on release probability and paired-pulse ratio. However, cultures overexpressing SYD1A-mCherry (n=11 fields) showed no difference in release probability (**Fig. 8A**, p=0.422), paired-pulse ratio (**Fig. 8B**, p=0.536), or RRP size (**Fig. 8C**, p=0.774) when compared to controls (n=11 fields). Considering that we failed to

change the size of the RRP, our hypothesis concerning the independent modulation of P_r and RRP remains unresolved.

CHAPTER 4: DISCUSSION

4.1. OPTICAL MEASUREMENT OF PAIRED-PULSE PLASTICITY REVEALS CONSIDERABLE HETEROGENEITY OF PPR AMONG INDIVIDUAL PRESYNAPTIC NEURONS

The purpose of this study was to investigate the relationship between release probability and paired-pulse ratio at individual synapses. Our first aim was to measure paired-pulse ratio at isolated release sites using an optical sensor of vesicle exocytosis. Assessing paired-pulse ratio at individual synapses is often not possible with conventional electrophysiological measurements, which provide only population-averaged measurements of PPR from a set of synapses that converge onto a single postsynaptic neuron. We succeeded in measuring the paired-pulse ratio at individual synapses in hippocampal neurons transfected with sypHl, and were able to compare the PPR between synapses of a single axon, as well as between the synapses of different neurons.

The PPR values we measured with sypHl at synapses between hippocampal neurons were comparable to the values reported in earlier studies that relied on electrophysiology. At paired-pulse frequencies similar to the one used in our study (40 Hz), synapses made by associational/commissural afferents onto pyramidal neurons usually show moderate facilitation with a PPR between 1.5 and 2.5 (Creager et al., 1980; Salin et al., 1996), while mossy fiber synapses onto CA3 neurons facilitate more strongly (PPR between 2.5 and 4; Zalutsky and Nicoll., 1990; Salin et al., 1996; Contractor et al., 2001), and GABAergic synapses are overwhelmingly depressing (PPR around 0.5; McCarren and Alger, 1985; Wilcox and Dichter, 1994). The values we report for PPR at individual synapses (2.17±0.24, n=4 axons) are consistent with this previous work.

Furthermore, our values are highly similar to those reported in another study in which PPR was measured directly at individual hippocampal synapses (2.07±0.19, Murthy et al., 1997) through the use of FM dye. The agreement of our measurements with those reported in previous literature supports the validity of our novel method of measuring PPR.

There are several possible explanations for the large variability that we observed between the individual synapses of a single axon. First, it has been suggested that short-term plasticity at a synapse is partially regulated by its postsynaptic target. In hippocampal slice cultures, Schaffer collateral synapses onto interneurons have a smaller PPR than Schaffer collateral synapses onto CA1 pyramidal neurons (Sun et al., 2005). Similarly, mossy fibre synapses onto interneurons may be either facilitating or depressing, but mossy fibre synapses onto CA3 pyramidal neurons show only facilitation (Toth et al., 2000). Our cultures were generated from dissociated embryonic rat hippocampus and are therefore likely to contain a heterogeneous population of cells, including granule cells, CA1 and CA3 pyramidal neurons, and GABAergic interneurons. The potential variability in postsynaptic target may have influenced the PPR of individual synapses from the same presynaptic cell. A second possible explanation involves the dynamic change of short-term plasticity at a set of synapses. In the hippocampus, mossy fibre synapses onto CA3 pyramidal cells have been shown to exhibit reduced PPR following the induction of LTP (Zalutsky and Nicoll, 1990). Such use-dependent alterations in STP at individual synapses may account for the variability in PPR along a single presynaptic axon.

In conclusion, we have shown that use of sypHl is a reliable and convenient method to assess paired-pulse ratio at individual synapses of a single neuron. This ability has allowed us to investigate the relationship between release probability and paired-pulse ratio at isolated release sites.

4.2. RELEASE PROBABILITY AND PAIRED-PULSE PLASTICITY ARE MEDIATED BY OVERLAPPING, BUT NON-IDENTICAL, SETS OF MECHANISMS

The primary aim of our work was to investigate the relationship between release probability and paired-pulse ratio at the level of individual synapses. In measuring the average values of PPR from synapse pools of unknown size, an inverse relationship between these properties has been observed in many circumstances (Debanne et al., 1996; Murthy et al., 1997; Silver et al., 1998; Bender et al., 2009). We measured release probability and paired-pulse ratio of each synapse along a single sypHl-transfected axon in hippocampal culture, and were able to compare these values between individual release sites. We found that release probabilities and paired-pulse ratios are inversely correlated at the synapses of a single presynaptic neuron. However, this inverse correlation between P_r and PPR is relatively moderate, and we were able to identify many synapses with identical release probabilities that expressed widely different PPR values. This finding is surprising in light of the commonly held view that release probability and paired-pulse plasticity are modulated by the same mechanisms. We therefore proceeded to explore the relationships between paired-pulse plasticity and two distinct determinants of release probability, RRP size and vesicular release probability. We confirmed previous findings (Dobrunz and Stevens, 1997; Murthy et al., 2001) of a positive correlation between release probability and RRP size. Surprisingly, however, we did not

observe any correlation between paired-pulse ratio and RRP size at the synapses of a single presynaptic neuron. This suggests that the size of the readily releasable pool of synaptic vesicles has little, if any, influence on short-term plasticity and indicates that mechanisms regulating the size of the synaptic vesicle pool, for example by altering the size of the active zone (Murthy et al., 2001; Matz et al., 2010; Matkovic et al., 2013), elicit P_r changes that are independent of alterations in PPR.

In contrast to RRP size, the vesicular release probability has a strong inverse correlation with the paired-pulse ratio among synapses of an identified presynaptic neuron. In fact, the correlation between PPR and $\overline{vP_r}$ was significantly stronger than that between PPR and P_r. Our results suggest that the mechanisms that regulate vP_r also regulate both release probability and paired-pulse plasticity at synapses and likely contribute to the inverse relationship between P_r and PPR, and that this inverse relationship is weakened by influences of RRP size on P_r. It should be noted that, to address the relationship between paired-pulse plasticity and determinants of release probability, we calculated vesicular release probability as a ratio of release probability and RRP size. An underlying assumption of this approach is that all readily releasable SVs at a synapse have the same vesicular release probability. We are aware that this assumption likely represents an oversimplification. In fact, previous modeling and experimental studies indicate that synaptic vesicles within a single RRP have a heterogeneous distribution of vesicular release probabilities (Meinrenken et al., 2002; Scimemi and Diamond, 2012). Regardless, our approach allowed us to demonstrate a strong inverse relationship at individual synapses between PPR and what we have defined as mean vesicular release probability ($\overline{vP_r}$).

vP_r is determined by mechanisms modulating calcium channel density and conductance (Hoppa et al., 2012) as well as the spatial coupling of presynaptic calcium channels and readily releasable synaptic vesicles (reviewed in Eggermann et al., 2012). These mechanisms lead to variability in the apparent calcium sensitivity of synaptic vesicle exocytosis at individual synapses. In an approach to address which determinants of release probability affect paired-pulse plasticity at synapses, we therefore compared calcium sensitivity and paired-pulse plasticity at individual synapses. We were able to demonstrate that the apparent calcium sensitivity of vesicle exocytosis strongly correlates with PPR at individual synapses, indicating that mechanisms which alter calcium sensitivity may act to inversely regulate release probability and short-term plasticity.

In summary, our observations have led us to believe that of two sets of mechanisms regulating release probability, only one affects paired-pulse plasticity at synapses. In particular, mechanisms modulating the size of the RRP of synaptic vesicles might regulate the release probability of a synapse but do not influence paired-pulse ratio. Synapses with a small RRP have a lower initial release probability than those with a large RRP (**Fig. 9A1**); however, the paired-pulse ratio of both synapses may theoretically be the same if the changes in release probability during short-term plasticity are proportional to the initial release probability (**Fig. 9A2**). In contrast, synapses with comparable RRP sizes but widely different vesicular release probabilities are likely to show an inverse correlation between release probability and PPR due to large differences in the proportion of the change in release probability during short-term plasticity (**Fig. 9B**). It is therefore possible that, if vesicular release probability remains constant at a synapse, its release probability may be altered independently of paired-pulse ratio following a change in the

size of the readily releasable pool. This consideration may be of importance for electrophysiological studies that investigate changes in paired-pulse ratio to infer alterations in release probability, or a lack thereof. Furthermore, our proposal that changes in RRP size may theoretically alter the reliability of a synapse without changing PPR is conceptually important, as it identifies a presynaptic mechanism that is able to alter synaptic strength without affecting the way transmission is temporally integrated at that synapse. Therefore, together with mechanisms altering the calcium sensitivity of SV exocytosis, changes in RRP size may allow presynaptic neurons to exert fine control over synaptic transmission and its integration in the postsynaptic neuron.

4.4 NO ALTERATIONS OF RRP SIZE IN EXPERIMENTS TO INDUCE HOMEOSTATIC PLASTICITY

The final aim of our work was to identify experimental manipulations that would allow us to alter RRP size and demonstrate that the release probability of individual release sites can be changed without altering the paired-pulse ratio. This would provide strong evidence for the independent regulation of release probability and PPR at the level of individual synapses. The induction of homeostatic plasticity at synapses between hippocampal neurons in dissociated cultures by blockade of voltage-gated sodium channels may represent such an experimental manipulation that elicits a rise in P_r through an increase in the size of the RRP (Murthy et al., 2001). However, we did not observe any significant difference in the size of the RRP between TTX-treated cultures and controls. In response to chronic blockade of voltage-gated sodium channels, release probability tended to increase and PPR to be reduced, but neither of these trends reached significance. It is possible that chronic TTX treatment induces homeostatic plasticity

through modulation of vesicular release probability, in which case, we would expect to see inverse changes in release probability and PPR. This idea is supported by the results of a recent study (Zhao et al., 2011) that concluded that homeostatic changes in release probability were driven by altered presynaptic calcium influx. With a larger data set, we may be able to see a significant difference in the release probability and paired-pulse ratio between groups, supporting the outcome of the Zhao study. However, this would not address our original hypothesis regarding independent modulation of release probability and PPR through a change in RRP size, and so we did not pursue this line of experiments further.

It is also possible that we observed no change in RRP size because our method of chronic activity suppression failed to induce homeostatic plasticity at all synapses studied. Dissociated primary cultures are composed of glutamatergic pyramidal neurons and dentate gyrus granule cells, but also contain a small amount of inhibitory interneurons (usually between 10-25%). A recent study has shown that TTX-induced homeostatic plasticity occurs only at synapses of dentate gyrus granule cells onto proximal apical dendrites of CA3 pyramidal neurons (Lee et al., 2013). The analysis in our current study did not take cell type or location of synapses into consideration. Thus, major differences in the expression of homeostatic plasticity between cell types may account for our results. If this experiment were to be repeated in the future, I would suggest an identification of cell type with post-hoc immunolabelling, or the use of an organotypic slice preparation, to allow assessment of the effects of homeostatic plasticity on a more homogenous pool of synapses.

4.5 SYD1A EXPRESSION LEVEL DOES NOT INFLUENCE RRP SIZE

Finally, we altered the expression of mSYD1A in hippocampal culture with the intention to change the size of the RRP and investigate the effect of this change on release probability and paired-pulse ratio. In both *Drosophila* (Owald et al., 2010) and *C. elegans* (Hallam et al., 2002), a SYD1 homologue has been shown to localize in the presynaptic terminal. In the case of *Drosophila,* knockdown of the SYD1 homologue reduces the number of vesicles docked at the active zone (Owald et al., 2010). This relationship between SYD1 and vesicle pool extends to mammals, which possess two SYD1 homologs, mSYD1A and mSYD1B, transcribed from two different genes that likely arose via gene duplication. In mouse cerebellar neurons, mSYD1A expression is required for presynaptic assembly, and interference with its expression reduces the number of docked synaptic vesicles (Wentzel et al., 2013). The expression level of mSYD1A was therefore an appealing candidate for a mechanism by which we might alter the size of the RRP. However, we did not see a significant change in our hippocampal cultures following an shRNA mediated knockdown of mSYD1A, nor after mSYD1A overexpression. There are several possible explanations for this outcome.

With the transfection of an mSYD1A knockdown construct, we saw a non-significant trend towards reduced RRP size. A more efficient knockdown construct, or the use of multiple knockdown constructs to target mSYD1A and its homologue mSYD1B simultaneously, may allow for a larger reduction in expression that is sufficient to obtain a significant change in RRP size. Alternatively, an increase in the number of neurons from which we recorded may produce significant results.

Overexpression of mSYD1A did not increase the size of the RRP, and unlike our observations of mSYD1A knockdown, there was no identifiable trend towards a change following overexpression. It might be that mSYD1A already has very high expression levels at hippocampal synapses, and/or that mSYD1A overexpression does not alter the functional levels of this protein. It is believed that mSYD1A is a Rho GTPase activating protein (GAP) that facilitates GTP hydrolysis and subsequently inactivates RhoA (Wentzel et al., 2013). Therefore, a major function of mSYD1A may be the local regulation of monomeric G proteins such as RhoA, and this function may already be carried out very effectively by endogenous levels of mSYD1A at the synapse. It is also possible that mSYD1A is not effectively targeted to presynaptic specializations. For example, sites of SYD1 binding to the presynaptic scaffolding protein alpha-liprin may be saturated with endogenous levels of this protein. Thus, the overexpression of mSYD1A would fail to cause a further increase in RhoA inactivation at presynaptic specializations.

In summary, our attempts to alter mSYD1A function to modulate RRP size have failed. If similar attempts were employed in the future to assess the relationship between RRP size and paired-pulse ratio, it would be wise to use mSYD1A knockdown constructs with greater effectiveness, or to reduce expression of mSYD1A and mSYD1B in combination.

4.6 CONCLUSION

In our research, we successfully employed a genetically encoded sensor of synaptic vesicle exocytosis to measure paired-pulse ratio at the individual synapses of a

single axon in hippocampal culture. We observed that the average PPR values within a field are comparable to the average measurements obtained using other methods. We were also able to witness a large amount of variability in PPR between synapses of optically identified presynaptic neurons, which has not been possible with previously used methods. This novel approach to measuring PPR allowed us to investigate the regulation of short-term plasticity at the level of individual release sites. Our work has confirmed previous findings of a negative correlation between release probability and paired-pulse ratio. However, we also have provided evidence the paired-pulse ratio is not associated with the size of the readily releasable pool of synaptic vesicles, suggesting that alterations in RRP size may correspond to changes in P_r that are independent of changes in PPR. Unfortunately, our initial efforts to manipulate the size of the readily releasable pool to modulate P_r independently of PPR were unsuccessful, and so further work is required to test this hypothesis more conclusively.

REFERENCES

Abbott, L.F. and Regehr, W.G. (2004) Synaptic computation. *Nature* 431(7010):796-803

Acuna, C., Guo, Q., Burré, J., Sharma, M., Sun, J. and Südhof, T.C. (2014) Microsecond dissection of neurotransmitter release: SNARE-complex assembly dictates speed and Ca2+ sensitivity. *Neuron* 82(5):1088-1100

Allen, C. and Stevens, C.F. (1994) An evaluation of causes for unreliability of synaptic transmission. *PNAS* 91: 10380-10383

Araya, R., Vogels, T.P. and Yuste, R. (2014) Activity-dependent dendritic spine neck changes are correlated with synaptic strength. *PNAS* 111(28):E2895-904

Ascher, P. and Nowak, L. (1988) THe role of divalent cations in the N-methyl-D-aspartate responses of mouse central neurones in culture. *J Phyisol* 399:247-266

Atluri, P.P. and Regehr, W.G. (1996) Determinants of the time course of facilitation at the granule cell to Purkinje cell synapse. *J Neurosci* 16(18):5661-71

Augustin, I., Rosenmund, C., Südhof, T.C. and Brose, N. (1999) Munc13-1 is essential for fusion competence of glutamatergic synaptic vesicles. *Nature* 400(6743):457-61

Baldelli, P., Hernandez-Guijo, J.M., Carabelli, V. and Carbone, E. (2005) Brain-derived neurotrophic factor enhances GABA release probability and nonuniform distribution of N- and P/Q-type channels on release sites of hippocampal inhibitory synapses. *J Neurosci* 25:3358-3368

Bao, J.X., Kandel, E.R. and Hawkins, R.D. (1997) Involvement of pre- and postsynaptic mechanisms in posttetanic potentiation at Aplysia synapses. *Science* 275(5302):969-973

Basarsky, T.A., Parpura, V., and Haydon, P.G. (1994) Hippocampal synaptogenesis in cell culture: developmental time course of synapse formation, calcium influx, and synaptic protein distribution. *J Neurosci* 14(11):6402-11

Bean, B.P. (1989) Neurotransmitter inhibition of neuronal calcium currents by changes in calcium voltage dependence. 340(6229):153-156

Bender, V.A., Pugh, J.R. and Jahr, C.E. (2009) Presynaptically expressed long-term potentiation increases multivesicular release at parallel fiber synapses *J Neurosci* 29: 10974-10978

Benke, T.A., Lüthi, A., Isaac, J.T.R. and Collingridge G.L. (1998) Modulation of AMPA receptor unitary conductance by synaptic activity. *Nature* 393:793-797

Bergsman, J.B., Krueger, S.R., and Fitzsimonds, R.M. (2006) Automated criteria-based selection and analysis of fluorescent synaptic puncta. *J Neurosci Methods* 152(1-2):32-39

Betz, W.J. (1970) Depression of transmitter release at the neuromuscular junction of the frog. *J Physiol* 206(3):629-644

Betz, A., Thakur, P., Junge, H.J., Ashery, U., Rhee, J.S., Scheuss, V., Rosenmund, C., Rettig, J. and Brose, N. (2001) Functional interaction of the active zone proteins Munc13-1 and RIM1 in synaptic vesicle priming. *Neuron* 30(1):183-96

Bi, G.Q. and Poo, M.M. (1998). Synaptic modifications in cultured hippocampal neurons: dependence on spike timing, synaptic strength, and postsynaptic cell type. 18(24):10464-72

Bliss, T.V.P. and Collingridge, G.L. (1993) A synaptic model of memory: long-term potentiation in the hippocampus *Nature* 361: 31-39

Bliss, T.V.P. and Lomo, T. (1973) Long lasting potentiation of synaptic transmission in the dentate area of the anaesthetized rabbit following stimulation of the perforant path. *J Physiol* 232: 331-356

Branco, T., Marra, V. and Staras, K. (2010) Examining size-strength relationships at hippocampal synapses using an ultrastructural measurement of synaptic release probability. *J Struct Biol* 172:203-210

Brody, D.L. and Yue, D.T. (2000) Release-independent short-term synaptic depression in cultured hippocampal neurons. *J Neurosci* 20(7):2480-2494

Cao, Y.Q. and Tsien, R.W. (2010) Different relationship of N- and P/Q-type Ca2+ channels to channel-interacting slots in controlling neurotransmission at cultured hippocampal synapses. *J Neurosci* 30(13):4536-46

Carroll, R.C., Lissin, D.V., von Zastrow, M., Nicoll, R.A. and Malenka, R.C. (1999) Rapid redistribution of glutamate receptors contributes to long-term depression in hippocampal cultures. *Nature Neuroscience* 2:454-460

Collingridge, G.L., Kehl, S.J. and McLennan, H. (1983) Excitatory amino acids in synaptic transmission in the Schaffer collateral-commissural pathway of the rat hippocampus *J Physiol* 334:33-46

Contractor, A., Swanson, H. and Heinemann, S.F. (2001) Kainate receptors are involved in short- and long-term plasticity at mossy fiber synapses in the hippocampus. *Neuron* 29(1):209-16

Creager, R., Dunwiddie, T. and Lynch, G. (1980) Paired-pulse and frequency facilitation in the CA1 region of the in vitro rat hippocampus. *J Physiol* 299:409-24

Davis, G.W. and Murphey, R.K. (1993) A role for postsynaptic neurons in determining presynaptic release properties in the cricket CNS: evidence for retrograde control of facilitation. *J Neurosci* 13(9):3827-38

Davis, G.W. (2013) Homeostatic signaling and the stabilization of neural function *Neuron* 80:718-728

Debanne, D., Gahwiler, B.H. and Thompson, S.M. (1994) Asynchronous pre- and postsynaptic activity induces associative long-term depression in area CA1 of the rat hippocampus in vitro. *roc Natl Acad Sci* 91(3):1148-1152

Debanne, D., Guérineau, N.C., Gähwiler, B.H. and Thompson, S.M. (1996) Paired-pulse facilitation and depression at unitary synapses in rat hippocampus: quantal fluctuation affects subsequent release *J Physiol* 491: 163-176

Derkach, V., Barria, A. and Soderling, T.R. (1999) Ca2+/calmodulin-kinase II enhances channel conductance of alpha-amino-3-hydroxy-5-methyl-4-isoxazolepropionate type glutamate receptors. *PNAS* 96:3269-3274

Desmond, N.L. and Levy, W.B. (1986) Changes in the postsynaptic density with long-term potentiation in the dentate gyrus. *J Comp Neurol* 253(4):476-82

Dittman, J.S. and Regehr, W.G. (1998) Calcium dependence and recovery kinetics of presynaptic depression at the climbing fiber to Purkinje cell synapse. *J Neurosci* 18:6147-6162

Dittman, J.S., Kreitzer, A.C. and Regehr, W.G. (2000) Interplay between facilitation, depression, and residual calcium at three presynaptic terminals. 20:1374-1385

Dobrunz, L. E. and Stevens, C. F. (1997) Heterogeneity of release probability, facilitation, and depletion at central synapses. *Neuron* 18: 995-1008

Dolphin, A.C., Errington, M.L. and Bliss, T.V.P. (1982) Long-term potentiation of the perforant path *in vivo* is associated with increased glutamate release. *Nature* 297:496-497

Dunlap, K. and Fischbach, G.D. (1978) Neurotransmitters decrease the calcium component of sensory neurone action potentials *Neuron* 276(5690):837-9

Eggermann, E., Bucurenciu, I., Goswami, S.P., and Jonas, P. (2012) Nanodomain coupling between Ca2+ channels and sensors of exocytosis at fast mammalian synapses. *Nat Rev Neurosci* 13(1):7-21

El-Husseini A.E., Schnell, E., Chetkovich, D.M., Nicoll, R.A. and Bredt, D.S. (2000) PSD-95 involvement in maturation of excitatory synapses. *Science* 290: 1364-1368

Emptage, N., Bliss, T.V.P., Fine, A. (1999) Single synaptic events evoke NMDA receptor-mediated release of calcium from internal stores in hippocampal dendritic spines. *Neuron* 22(1):115-124

Emptage, N.J., Reid, C.A., Fine, A., Bliss, T.V.P. (2003) Optical quantal analysis reveals a presynaptic component of LTP at hippocampal Schaffer-associational synapses. *Neuron* 38: 797-80

Engert, F. and Bonhoeffer, T. (1999) Dendritic spine changes associated with hippocampal long-term synaptic plasticity. *Nature* 399(6731):66-70

Enoki, R., Hu, Y.L., Hamilton, D. and Fine, A. (2009) Expression of long-term plasticity at individual synapses in hippocampus is graded, bidirectional and mainly presynaptic: optical quantal analysis. *Neuron* 62: 242-253

Ermolyuk, Y.S., Alder, F.G., Henneberger, C., Rusakov, D.A., Kullmann, D.M., and Volynski, K.E. (2012) Independent regulation of basal neurotransmitter release efficacy by variable Ca2+ influx and bouton size at small central synapses. *PLoS Biol* 10(9) doi:10.1371/journal.pbio.1001396

Fedchyshyn, M.J. and Wang, L.Y. (2005) Developmental transformation of the release modality at the calyx of Held synapse. *J Neurosci* 25:4131-4130

Felmy, F., Neher, E., and Schneggenburger, R. (2003) Probing the intracellular calcium sensitivity of transmitter release during synaptic facilitation. *Neuron* 37(5):801-11

Fioravante, D. and Regehr, W.G. (2011) Short-term forms of presynaptic plasticity. *Curr Opinion Neurobiol* 21(2):269-74

Fortune, E.S. and Rose, G.J. (2001) Short-term synaptic plasticity as a temporal filter. *Trends Neurosci* 24(7):381-5

Fuhrmann G., Segev, I., Markran, H., and Tsodyks, M. (2002) Coding of temporal information by activity-dependent synapses. *J Neurophysiol* 87(1):140-8

Futai, K., Kim, M.J., Hashikawa, T., Scheiffele, P., Sheng, M. and Hayashi, Y. (2007) Retrograde modulation of presynaptic release probability through signalling mediated by PSD-95-neuroligin. *Nat Neurosci* 10(2): 186-195

Gaffield. M.A. and Betz, W.J. (2007) Synaptic vesicle mobility in mouse motor nerve terminals with and without synapsin. *J Neurosci* 27(50): 13691-700

Gerber, S.H., Rah, J., Min, S., Liu, X., de Wit, H., Dulubova, I., Meyer, A.C., Rizo, J., Arancillo, M., Hammer, R.E., Verhage, M., Rosenmund, C. and Südhof, T.C. (2008) Conformational switch of syntaxin-1 controls synaptic vesicle fusion. *Science* 321(5895):1507-10

Goold, C.P. and Nicoll, R.A. (2010) Single-cell optogenetic excitation drives homeostatic synaptic depression *Neuron* 68(3):512-538

Granger, A.J. and Nicoll, R.A. (2013) Expression mechanisms underlying long-term potentiation: a postsynaptic view, 10 years on. *Philos Trans R Lond B Biol Sci* 369:20130136 doi: 10.1098/rstb.2013.0136

Granseth, B., Odermatt, B., Royle, S.J. and Lagnado, L. (2006) Clathrin-mediated endocytosis is the dominant mechanism of vesicle retrieval at hippocampal synapses. *Neuron* 51(6):773-786

Grosshans, D.R., Clayton, D.A., Coultrap, S.J. and Browning, M.D. (2002) LTP leads to rapid surface expression of NMDA but not AMPA receptors in adult rat CA1. *Nat Neurosci* 5(1):27-33

Hallam, S.J., Goncharov, A., McEwen, J., Baran, R. and Jin, Y. (2002) SYD-1, a presynaptic protein with PDZ, C2 and rhoGAP-like domains, specifies axon identity in C. elegans. *Nat Neurosci* 5(11):1137-46

Han, Y., Kaeser, P.S., Sudhof, T.C. and Schneggenburger, R. (2011) RIM determines Ca2+ channel density and vesicle docking at the presynaptic active zone. 69(2):304-16

Harris, E.W. and Cotman, C.W. (1986) Long-term potentiation of guinea pig mossy fiber responses is not blocked by N-methyl-D-aspartate antagonists *Neurosci Lett* 70:132-137

Harris, K.M. and Stevens, J.K. (1989) Dendritic spines of CA1 pyramidal cells in the rat hippocampus: serial electron microscopy with reference to their biophysical characteristics. *J Neurosci* 9(8): 2982-2997

Hata, Y., Slaughter, C.A. and Südhof, T.C. (1993) Synaptic vesicle fusion complex contains unc-18 homologue bound to syntaxin. *Nature* 366(6453):347-351

Hatt, H. and Smith, D.O. (1976) Synaptic depression related to presynaptic axon conduction block. *J Physiol* 259(2):367-93

Hessler, N.A., Shirke, A.M. and Malinow, R. (1993) The probability of transmitter release at a mammalian central synapse. *Nature* 366: 569-572

Holderith, N., Lorincz, A., Katona, G., Rózsa, B., Kulik, A., Watanabe, M., Nusser, Z. (2012) Release probability of hippocampal glutamatergic terminals scales with size of the active zone. *Nat Neurosci* 15:988-997

Holz, G.G. 4th, Rane, S.G. and Dunlap, K. (1986) GTP-binding proteins mediate transmitter inhibition of voltage-dependent calcium channels. 319(6055): 670-672

Hoppa, M.B., Lana, B., Margas, W., Dolphin, A.C. and Ryan, T.A. (2012) α2δ expression sets presynaptic calcium channel abundance and release probability *Nature* 486(7401):122-125

Hosoi, N., Sakaba, T. and Neher, E. (2007) Quantitative analysis of calcium dependent vesicle recruitment and its functional role at the calyx of Held synapse. *J Neurosci* 27:14286-14298

Hou, Q., Zhang, D., Jarzylo, L., Huganir, R.L. and Man, H.Y. (2008) Homeostatic regulation of AMPA receptor expression at single hippocampal synapses. *Proc Natl Acad Sci USA* 105(2):775-780

Hsia, A.Y., Malenka, R.C. and Nicoll, R.A. (1998) Development of excitatory circuitry in the hippocampus. *J Neurophysiol* 79(4):2013-24

Hsu, S.F., Augustine, G.J. and Jackson, M.B. (1996) Adaptation of Ca(2+) triggered exocytosis in presynaptic terminals. *Neuron* 17(3):501-512

Ibata, K., Sun, Q. and Turrigiano, C.G. (2008) Rapid synaptic scaling induced by changes in postsynaptic firing *Neuron* 57(6):819-826

Isaac, J.T., Nicoll, R.A. and Malenka, R.C. (1995) Evidence for silent synapses: implications for the expression of LTP. *Neuron* 15(2): 427-434

Isaac, J.T., Oliet, S.H., Hjelmstad, G.O., Nicoll, R.A. and Malenka, R.C. (1996) *J Physiol Paris* 90: 299-303

Ito, I. and Sugiyama, H. (1991) Roles of glutamate receptors in long-term potentiation at hippocampal mossy fiber synapses *Neuroreport* 2:333-336

Junge, H.J., Rhee, J.S., Jahn O., Varoqueaux, F., Spiess, J., Waxham, M.N., Rosenmund, C., and Brose, N. (2004) Calmodulin and Munc13 form a Ca2+ sensor/effector complex that controls short-term synaptic plasticity. *Cell* 118(3):389-401

Kamiya, H. and Zucker, R.S. (1994) Residual Ca2+ and short-term synaptic plasticity. 371(6498):603-6

Kamiya, H., Ozawa, S., and Manabe, T. (2002) Kainate receptor-dependent short-term plasticity of presynaptic Ca2+ influx at the hippocampal mossy fiber synapses. *J Neurosci* 22(21):9237-43

Kaeser, P.S., Deng, L., Wang, Y., Dulubova, I., Liu, X., Rizo, J., Südhof, T.C. (2011) RIM proteins tether Ca2+ channels to presynaptic active zones via a direct PDZ-domain interaction. *Cell* 144(2):282-95

Kavalali. E.T. and Jorgensen, E.M. (2014) Visualizing presynaptic function. *Nat N eurosci* 17:10-16

Kristensen, A.S., Jenkins, M.A., Banke, T.G., Schousboe, A., Makino, Y., Johnson, R.C., Huganir, R., Traynelis, S.F. (2011) Mechanism of Ca2+/calmodulin-dependent kinase II regulation of AMPA receptor gating *Nat Neurosci* 14(6):727-735

Kopec, C.D., Real, E., Kessels, H.W. and Malinow, R. (2007) GluR1 links structural and functional plasticity at excitatory synapses. *J Neurosci* 27(50):13706-18

Kravchenko, M.O., Moskalyuk, A.O., Fedulova, S.A. and Veselovsky, N.S. (2006) Calcium-dependent changes of paired-pulse modulation at single GABAergic synapses. *Neurosci Lett* 395(2):133-7

Kullmann, D.M. (1994) Amplitude fluctuations of dual-component EPSCs in hippocampal pyramidal cells: implications for long-term potentiation. *Neuron* 12(5):1111-20

Kusano, K. and Landau, E.M. (1975) Depression and recovery of transmission at the squid giant synapse. *J Physiol* 245(1):13-32

Lazarevic, V., Schöne, C., Heine, M., Gundelfinger, E.D. and Fejtova, A. (2011) Extensive remodeling of the presynaptic cytomatrix upon homeostatic adaptation to network silencing *J Neurosci* 31:10189-101200

Lazarevic, V., Pothula, S., Andres-Alonso, M. and Fejtova, A. (2013) Molecular mechanisms driving homeostatic plasticity of neurotransmitter release *Front Cell Neurosci* 7:244 doi:10.3389/fncel.2013.00244

Leal, K., Mochida, S., Scheuer, T., and Catterall, W.A. (2012) Fine-tuning synaptic plasticity by modulation of Ca(V)2.1 channels with Ca2+ sensor proteins. *Proc Natl Acad Sci USA* 109(42):17069-17074

Lee, H.K., Kameyama, K., Huganir, R.L. and Bear, M.F. (1998) NMDA induces long-term synaptic depression and dephosphorylation of the GluR1 subunit of AMPA receptors in hippocampus. *Neuron* 21:1151-1162

Lee, A., Wong, S.T., Gallagher, D., Li, B., Storm, D.R., Scheuer, T. and Catterall, W.A. (1999) Ca2+/calmodulin binds to and modulates P/Q-type calcium channels. *Nature* 399(6732):155-9

Liao, D., Hessler, N.A. and Malinow, R. (1995) Activation of postsynaptically silent synapses during pairing-induced LTP in CA1 region of hippocampal slice. *Nature* 375(6530):400-404

Lissin, D.V., Gomperts, S.N., Carroll, R.C., Christine, C.W., Kalman, D., Kitamura, M., Hardy, S., Nicoll, R.A., Malenka, R.C. and von Zastrow, M. (1998) Activity differentially regulates the surface expression of synaptic AMPA and NMDA glutamate receptors *Proc Natl Acad Sci USA* 95:7097-7102

Lynch, G., Larson, J., Kelso, S., Barrionuevo, G. and Schottler, F. (1983) Intracellular injections of EGTA block induction of hippocampal long-term potentiation *Nature* 305: 719-721

Maletic-Savatic, M., Malinow, R. and Svoboda, K. (1999) Rapid dendritic morphogenesis in CA1 hippocampal dendrites induced by synaptic activity. 283(5409):1923-1927

Malinow, R. and Malenka, R.C. (2002) AMPA receptor trafficking and synaptic plasticity *Annu Rev Neurisci* 25: 103-126p

Matkovic, T., Siebert, M., Knoche, E., Depner, H., Mertel, S., Oswald, D., Schmidt, M., Thomas, U., Sickmann, A., Kamin, D., Hell, S.W., Bürger, J., Hollmann, C., Mielke, T., Wichmann, C. and Sigrist, S.J. (2013) The Bruchpilot cytomatrix determines the size of the readily releasable pool of synaptic vesicles. *J Cell Biol* 202:667-683

Matsuzaki, M., Honkura, N., Ellis-Davies, G.C.R and Kasai, H. (2004) Structural basis of long-term potentiation in single dendritic spines. *Nature* 429: 761-766

Matz, J., Gilyan, A., Kolar, A., McCarvill, T. and Krueger, S.R. (2010) Rapid structural alterations of the active zone lead to sustained changes in neurotransmitter release *PNAS* 107: 8836-8841

McCarren. M. and Alger, B.E. (1985) Use-dependent depression of IPSPs in rat hippocampal pyramidal cells in vitro. *J Neurophysiol* 53(2):557-71

McEwen, J.M., Madison, J.M., Dybbs, M., and Kaplan, J.M. (2006) Antagonistic regulation of synaptic vesicle priming by Tomosyn and UNC-13. *Neuron* 51(3):303-15

Meinrenken, C.J., Borst, J.G., and Sakmann, B. (2002) Calcium secretion coupling at calyx of held governed by nonuniform channel-vesicle topography. 22(5):1648-1667

Mellor. J. and Nicoll, R.A. (2001) Hippocampal mossy fibre LTP is independent of postsynaptic calcium. *Nat Neurosci* 4(2):125-126

Mennerick, S. and Zorumski, C.F. (1995) Presynaptic influence on the time course of fast excitatory synaptic currents in cultured hippocampal cells. *J Neurosci* 15(4):3178-92

Meyer, A.C., Neher, E. and Schneggenburger, R. (2001) Estimation of quantal size and number of functional active zones at the calyx of held synapse by nonstationary EPSC variance analysis. *J Neurosci* 21:7889-7900

Meyer, D., Bonhoeffer, T., Scheuss, V. (2014) Balance and stability of synaptic structures during synaptic plasticity. *Neuron* 82(2):430-43

Miesenböck, G., De Angelis, D.A. and Rothman, J.E. (1998) Visualizing secretion and synaptic transmission with pH-sensitive green fluorescent proteins *Nature* 394(6689):1920195

Mochida, S., Few, A.P., Scheuer, T. and Catterall, W.A. (2008) Regulation of presynaptic Ca(V)2.1 channels by Ca2+ sensor proteins mediates short-term synaptic plasticity. 57(2):210-216

Montgomery, J.M. and Madison, D.V. (2002) State-dependent heterogeneity in synaptic depression between pyramidal cell pairs *Neuron* 33:765-777

Muller, M., Liu, K.S., Sigrist, S.J. and Davis, G.W. (2012) RIM controls homeostatic plasticity through modulation of the readily-releasable vesicle pool *J Neurosci* 32(47): 16574-16585

Murthy, V.N., Sejnowski, T.J. and Stevens, C.F. (1997) Heterogeneous release properties of visualized individual hippocampal synapses. *Neuron* 18: 599-612

Murthy, V.N., Schikorski, T., Stevens, C.F. ad Zhu, Y. (2001) Inactivity produces increases in neurotransmitter release and synapse size. *Neuron* 32: 673-682

Nägerl, U.V., Eberhorn, N., Cambridge, S.B. and Bonhoeffer, T. (2004) Bidirectional activity-dependent morphological plasticity in hippocampal neurons. *Neuron* 44(5):759-767

Nicoll, R.A. and Malenka, R.C. (1995) Contrasting properties of two forms of long-term potentiation in the hippocampus *Nature* 377:115-118

Nowak, L., Bregestovski, P., Ascher, P., Herbet, A. and Prochiantz, A. (1984) Magnesium gates glutamate-activated channels in mouse central neurones *Nature* 307:462-465

O'Brien, R.J., Kamboj, S., Ehlers, M.D., Rosen, K.R., Fischbach, G.D., Huganir, R.L. (1998) Activity-dependent modulation of synaptic AMPA receptor accumulation *Neuron* 21(5):1067-1078

Owald, D., Fouquet, W., Schmidt, M., Wichmann, C., Mertel, S., Depner, H., Christiansen, F., Zube, C., Quentin, C., Körner, J., Urlaub, H., Mechtler, K. and Sigrist, S.J. (2010) A Syd-1 homologue regulates pre- and postsynaptic maturation in Drosophila. *J Cell Biol* 188(4):565-79

Pan, B., Yang, D.W., Han, T.Z., and Xie, W. (2004) Changes in the paired-pulse ratio after long-term potentiation induced by 2- and 100-Hz tetanus in rat visual cortical slices. 1021(1):146-50

Patil, P.G., Brody, D.L. and Yu, D.T. (1998) Preferential closed-state inactivation of neuronal calcium channels. *Neuron* 20(5):1027-1038

Pawlak, V., Schupp, B.J., Single, F.N., Seeburg, P.H., Köhr, G. (2005) Impaired synaptic scaling in mouse hippocampal neurones expressing NMDA receptors with reduced calcium permeability. *J Physiol* 562:771-783

Petralia, R.S., Esteban, J.A., Wang, Y.X., Partridge, J.G., Zhao, H.M., Wenthold, R.J. and Malinow, R. (1999) Selective acquisition of AMPA receptors over postnatal development suggests a molecular basis for silent synapses. *Nat Neurosci* 2(1): 31-36

Pickard, L., Noël, J., Duckworth, J.K., Fitzjohn, S.M., Henley, J.M., Collingridge, G.L. and Molnar, E. (2001) Transient synaptic activation of NMDA receptors leads to the insertion of native AMPA receptors at hippocampal neuronal plasma membranes *Neuropharmacology* 41: 700-13

Pierce, J.P. and Mendell, L.M (1993) Quantitative ultrastructure of Ia boutons in the ventral horn: scaling and positional relationships. *J Neurosci* 13:4748-4743

Rausche, G., Sarvey, J.M., and Heinemann, U. (1988) Lowering extracellular calcium reverses paired pulse habituation into facilitation in dentate granule cells and removes a late IPSP. *Neurosci Lett* 88(3):275-80

Regehr, W.G., Delaney, K.R. and Tank, D.W. (1994) The role of presynaptic calcium in short-term enhancement at the hippocampal mossy fiber synapse *J Neurosci* 14:523-537

Reid, C.A., Dixon, D.B., Takahashi, M., Bliss, T.V. and Fine, A. (2004) Optical quantal analysis indicates that long-term potentiation at single hippocampal mossy fiber synapses is expressed through increased release probability, recruitment of new release sites, and activation of silent synapses. *J Neurosci* 24: 3618-3626

Richmond, J.E., Weimer, R.M., and Jorgensen, E.M. (2001) An open form of syntaxin bypasses the requirement for UNC-13 in vesicle priming. *Nature* 412:338-41

Rosenmund, C., Clements, J.D. and Westbrook, G.L. (1993) Nonuniform probability of glutamate release at hippocampal synapses *Science* 262: 754-757

Rosenmund, C. and Stevens, C.F. (1996) Definition of the readily-releasable pool of vesicles at hippocampal synapses. *Neuron* 16(6):1197-1207

Rosenmund, C., Sigler, A., Augustin, I., Reim, K., Brose, N. and Rhee, J.S. (2002) Differential control of vesicle priming and short-term plasticity by Munc13 isoforms. *Neuron* 33(3):411-24

Salin, P.A., Scanziani, M., Malenka, R.C., and Nicoll, R.A. (1996) Distinct short-term plasticity at two excitatory synapses in the hippocampus. *Proc Natl Acad Sci USA* 93(23):13304-9

Sankaranarayanan, S. and Ryan, T.A. (2000) Real-time measurements of vesicle-SNARE recycling in synapses of the central nervous system. *Nat Cell Biol* 2:197-204

Schikorski, T. and Stevens, C.F. (1997) Quantitative ultrastructural analysis of hippocampal excitatory synapses. *J Neurosci* 17:5858-5867

Schikorski, T. and Stevens, C.F. (2001) Morphological correlates of functionally defined synaptic vesicle populations. *Nat Neurosci* 4(4):391-5

Schneggenburger, R., Meyer, A.C., and Neher, E. (1999) Released fraction and total size of a pool of immediately available transmitter quanta at a calyx synapse. *Neuron* 23(2):399-409

Schneggenburger, R., Sakaba, T. and Neher, E. (2002) Vesicle pools and short-term synaptic depression: lessons from a large synapse. 25(4):206-12

Scimemi, A., and Diamond, J.S. (2012) The number and organization of Ca2+ channels in the active zone shapes neurotransmitter release from Schaffer collateral synapses. *J Neurosci* 32(50):18157-76

Scoville, W., and Milner, B. (1957). Loss of recent memory after bilateral hippocampal lesions. *J Neurol Neurosur PS* 20(1):11-21

Sheng, J., He, L., Zheng, H., Xue, L., Luo, F., Shin, W., Sun, T., Kuner, T., Yue, D.T. and Wu, L.G. (2012) Calcium channel number critically influences synaptic strength and plasticity at the active zone. *Nat Neurosci* 15:990-1006

Shi, S.H., Hayashi, Y., Petralia, R.S., Zaman, S.H., Wenthold, R.J., Svoboda, K. and Malinow, R. (1999) Rapid spine delivery and redistribution of AMPA receptors after synaptic NMDA receptor activation. *Science* 284: 1811-1816

Silver, R.A., Momiyama, A., Cull-Candy, S.G. (1998) Locus of frequency-dependent depression identified with multiple-probability fluctuation analysis at rat climbing fibre-Purkinje cell synapses. *J Physiol* 510:881-902

Stevens, C.F. and Wang, Y. (1994) Changes in reliability of synaptic function as a mechanism for plasticity. *Nature* 371:704-707

Stevens, C.F. and Wang, Y. (1995) Facilitation and depression at single central synapses *Neuron* 795-802

Südhof, T. C. (2012) The presynaptic active zone. *Neuron* 75:11-25

Sun, H.Y., Lyons, S.A. and Dobrunz, L.E. (2005) Mechanisms of target-cell specific short-term plasticity at Schaffer collateral synapses onto interneurones versus pyramidal cells in juvenile rats. *J Physiol* 568:815-40

Sun, Y.G., and Beierlein, M. (2011) Receptor saturation controls short-term synaptic plasticity at corticothalamic synapses, *J Neurophysiol* 105(5): 2319-2329

Talpalar, A.E., and Grossman, Y. (2003) Modulation of rat corticohippocampal synaptic activity by high pressure and extracellular calcium: single and frequency responses. *J Neurophysiol* 90(4):2106-14

Thiagarajan, T.C., Lindskog, M. and Tsien, R.W. (2005) Adaptation to synaptic inactivity in hippocampal neurons. *Neuron* 47: 725-737

Toth, K., Suares, G., Lawrence, J.J., Philips-Tansey, E. and McBain, C.J. (2000) Differential mechanisms of transmission at three types of mossy fiber synapse. *J Neurosci* 20(22):8279-89

Trussell, L.O. and Fischbach, G.D. (1989) Glutamate receptor desensitization and its role in synaptic transmission. *Neuron* 3(2):209-218

Turrigiano, G.G., Leslie, K.R., Desai, N.S., Rutherford, L.C. and Nelson, S.B. (1998) Activity-dependent scaling of quantal amplitude in neocortical neurons *Nature* 391: 892-896

Verhage, M., Maia, A.S., Plomp, J.J., Brussaard, A.B., Heeroma, J.H., Vermeer, H., Toonen, R.F., Hammer, R.E., van den Berg, T.K., Missler, M., Geuze, H.J. and Südhof, T.C. (2000) Synaptic assembly of the brain in the absence of neurotransmitter secretion. *Science* 287(5454):864-869

Waldeck, R.F., Pereda, A. and Faber, D.S. (2000) Properties and plasticity of paired-pulse depression at a central synapse 20:5312-5320

Wang, L.Y. and Kaczmarek, L.K. (1998) High frequency firing helps replenish the readily releasable pool of synaptic vesicles. *Nature* 394(6691): 384-388

Ward, B., McGuinness, L., Akerman, C.J., Fine, A., Bliss, T.V.P., Emptage, N.J. (2006) State-dependent mechanisms of LTP expression revealed by optical quantal analysis. *Neuron* 52:649-661

Weisskopf, M.G. and Nicoll, R.A. (1995) Presynaptic changes during mossy fibre LTP revealed by NMDA receptor-mediated synaptic responses. *Nature* 376:256-259

Wentzel, C., Sommer, J.E., Nair, R., Stiefvater, A., Sibarita, J. and Scheiffele, P. (2013) mSYD1A, a mammalian synapse-defective-1 protein, regulates synaptogenic signalling and vesicle docking. *Neuron* 78(6):1012-1023

Wierenga, C.J., Ibata, K., and Turrigiano, G.G. (2005) Postsynaptic expression of homeostatic plasticity at neocortical synapses. *J Neurosci* 25(11):2895-905

Wierenga, C.J., Walsh, M.F. and Turrigiano, G.G. (2006) Temporal regulation of the expression locus of homeostatic plasticity. *J Neurophysiol* 96: 2127-2133

Wigström, H., Gustafsson, B., Huang, Y.Y. and Abraham, W.C. (1986) Hippocampal long-term potentiation is induced by pairing single afferent volleys with intracellularly injected depolarizing current pulses *Acta Physiol Scand* 126: 317-319

Wilcox. K.S. and Dichter, M.A. (1994) Paired-pulse depression in cultured hippocampal neurons is due to a presynaptic mechanism independent of GABAB autoreceptor activation. *J Neurosci* 14:1775-88

Wu, L.G., Westenbroek, R.E., Borst, J.G., Catterall, W.A., Sakmann, B., (1999) Calcium channel types with distinct presynaptic localization couple differentially to transmitter release in single calyx-type synapses. *J Neurosci* 19(2):726-736

Wu, L.G. and Saggau, P. (1994) Presynaptic calcium is increased during normal synaptic transmission and paired-pulse facilitation, but not in long-term potentiation in area CA1 of hippocampus. 14(2):645-54

Xu, J. and Wu, L.G. (2005) The decrease in presynaptic calcium current is a major cause of short term depression at a calyx-type synapse. *Neuron* 46(4):633-645

Yang, Y.M., Fedchyshyn, M.J., Grande, G., Aitoubah, J., Tsang, C.W., Xie, H., Ackerley, C.A., Trimble, W.S. and Wang, L.Y. (2010) Septins regulate developmental switching from microdomain to nanodomain coupling of Ca2+ influx to neurotransmitter release at a central synapses. *Neuron* 67:100-115

Yeckel, M.F., Kapur, A., Johnston, D. (1999) Multiple forms of LTP in hippocampal CA3 neurons use a common postsynaptic mechanism. *Nat Neurosci* 2(7):625-33

Zalutsky, R.A. and Nicoll, R.A. (1990) Comparison of two forms of long-term potentiation in single hippocampal neurons *Science* 248: 1619-1624

Zengel, J.E. and Magleby, K.L. (1982) Augmentation and facilitation of neurotransmitter release. A quantitative description at the frog neuromuscular junction. *J Gen Physiol* 80(4): 583-611

Zilly, F.E., Sorensen, J.B., Jahn, R. and Lang, T. (2006) Munc18-bound syntaxin readily forms SNARE complexes with synaptobrevin in native plasma membranes. *PLoS Biol* 4(10):e330

Zhao, C., Dreosti, E. and Lagnado, L. (2011) Homeostatic synaptic plasticity through changes in presynaptic calcium influx 31:7492-7496

Zhou, Q., Homma, K.J. and Poo, M. (2004) Shrinkage of dendritic spines associated with long-term depression of hippocampal synapses. *Neuron* 44: 749-757

APPENDIX A: FIGURES

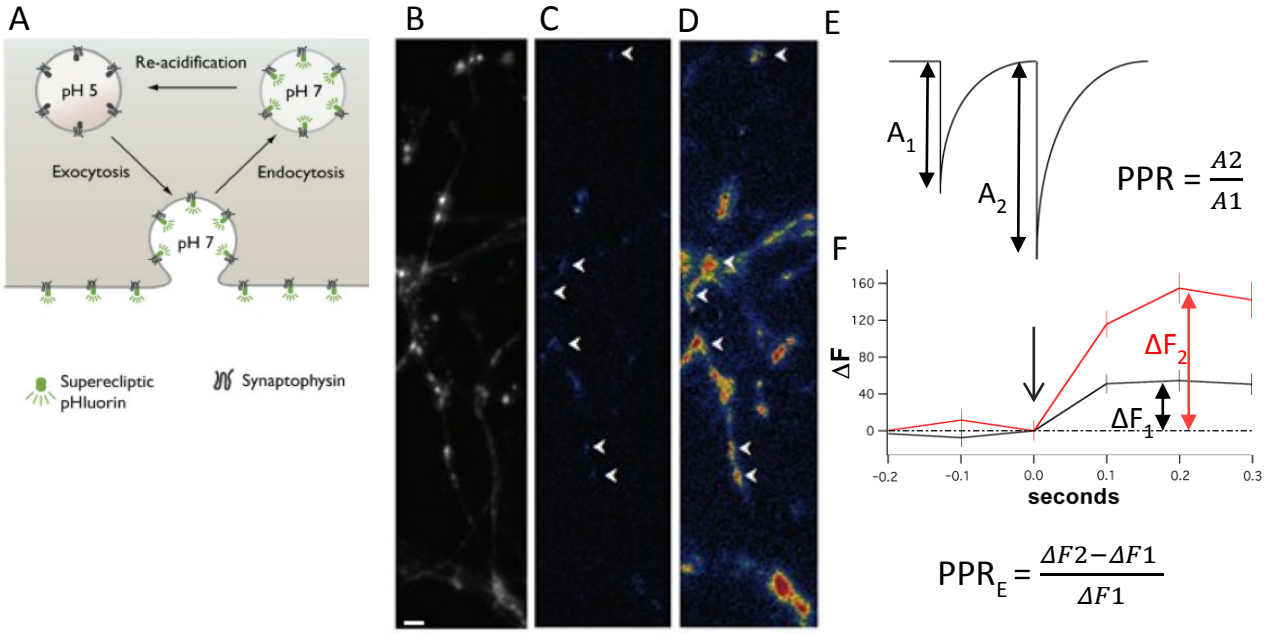

FIGURE 1. Synaptophysin-pHluorin is an optical sensor of vesicle exocytosis. (A) SypHl is a pH-sensitive fluorophore encoded in the vesicular lumen which produces an increase in fluorescence following exocytosis. (B) Basal fluorescence is visible in a single axon in dissociated hippocampal neuron culture that has been transfected with sypHl. Scale bar is 2 μm. Pseudo-color images were generated to represent the sum of the change in fluorescence in response to a 1ms square pulse field stimulation, (C) a change in response to paired-pulse stimuli (paired-pulse interval 25 msec) or (D) an 80 Hz, 2sec train of stimuli, and allow for the optical identification of synapses (white arrows). (E) A mock electrophysiological trace illustrates a common method for determining paired-pulse ratio. (F) Changes in sypHl fluorescence in response to single stimuli (black trace; responses at a single synapse averaged over 100 trials) or pairs of stimuli (red trace;

responses at the same synapse averaged over 100 trials) are used to approximate release probability and paired-pulse ratio. Downward arrow indicates stimulation.

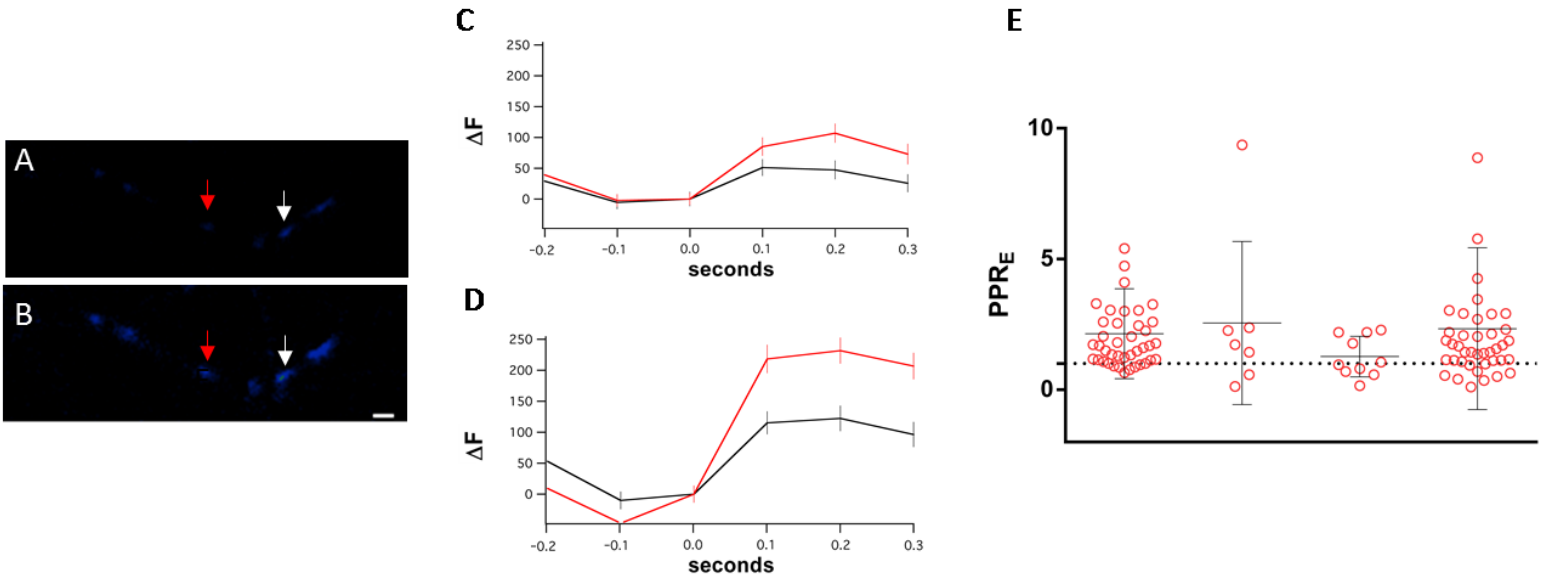

FIGURE 2. Paired-pulse ratio varies among synapses of a single axon Synaptic fluorescent responses to (A) a single stimulus and (B) pairs of stimuli (interpulse interval 25 msec) were used to calculate paired-pulse ratio for individual synapses along a single axon. Scale bar is 2 μm. Synapses showed considerable variability in PPR. Traces for single and paired responses of neighboring synapses are shown (C, traces for synapse identified by red arrow, PPR=2.60; D, traces for synapse identified by white arrow, PPR=1.14). (E) Plot of paired-pulse ratio for all synapses along each of four axons highlights the variability of PPR within a single neuron, as well as variability between neurons. Paired-pulse ratios of individual synapses (red circles) are shown with the mean and standard deviation of the distribution along each axon. The mean and standard deviation of the entire synaptic population are shown in bold. Dotted line represents a PPR value of 1.

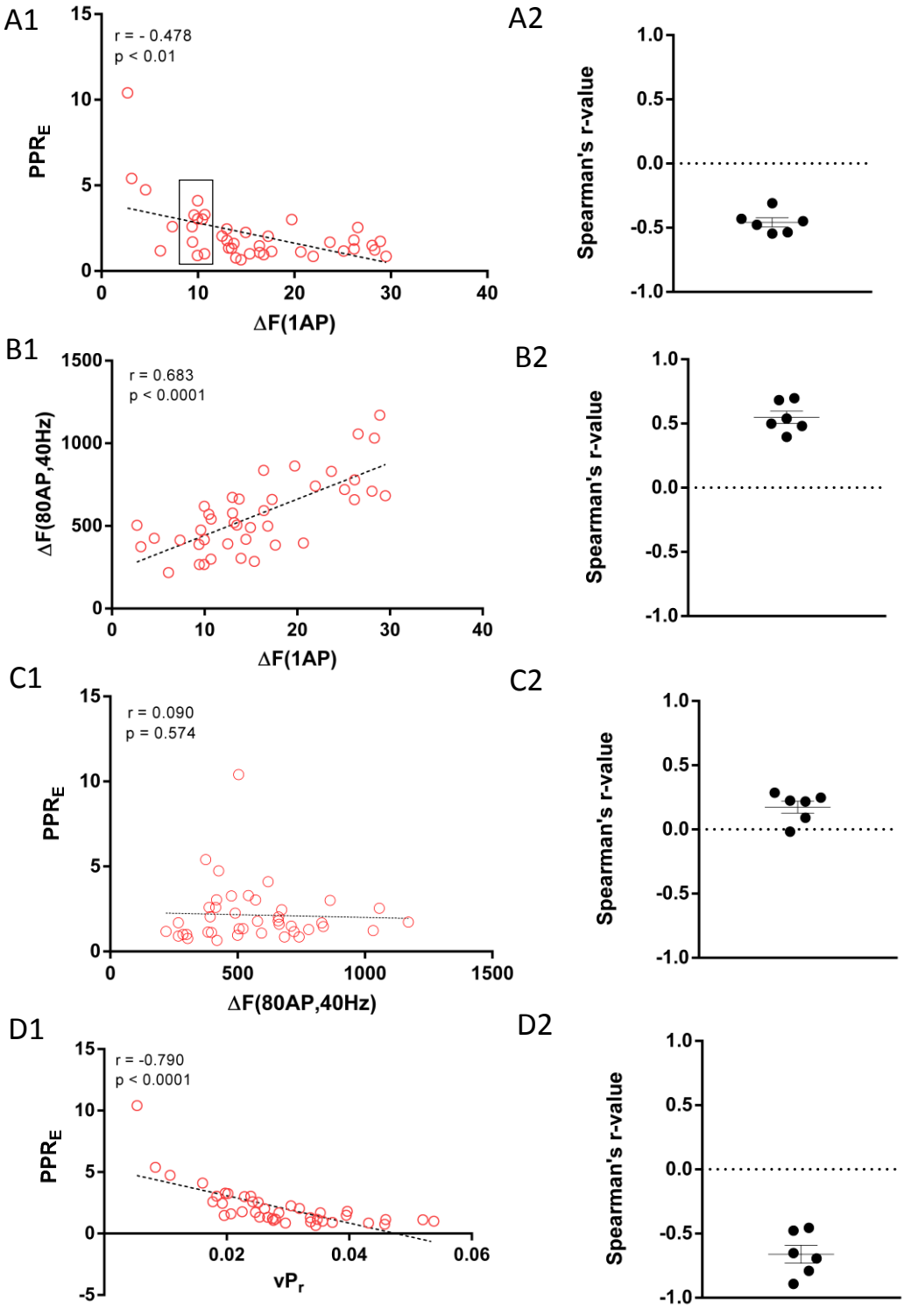
A1
r = - 0.478
p < 0.01
PPR_E
ΔF(1AP)
A2
Spearman's r-value
B1
r = 0.683
p < 0.0001
ΔF(80AP,40Hz)
ΔF(1AP)
B2
Spearman's r-value
C1
r = 0.090
p = 0.574
PPR_E
ΔF(80AP,40Hz)
C2
Spearman's r-value
D1
r = -0.790
p < 0.0001
PPR_E
vP_r
D2
Spearman's r-value

FIGURE 3. Summary of the correlations between properties at the synapses along individual axons. (A) The average increase in fluorescence at a synapse in response to a single action potential (ΔF(1AP)) is a measure of release probability for that synapse. Release probability and paired-pulse ratio are inversely correlated at the synapses of a single axon. This relationship is illustrated with a sample experiment showing data for all synapses of a single axon (A1) as well as a summary of Spearman's r-values for all experiments (A2, r_{av}= -0.458±0.035, n=6 axons). (B) The average increase in fluorescence at a synapse following a 40 Hz train of 80 stimuli (ΔF(80stim,40Hz)) is a measure of RRP size at that synapse. Release probability and RRP size are positively correlated at the synapses of a single axon (B1, sample experiment) for all experiments (B2, r_{av}= 0.550±0.048, n=6 axons). (C) Paired-pulse ratio and RRP size are not correlated at the synapses of a single axon (C1, sample experiment). There were no significant correlations between PPR and RRP size at any of the axons that were analyzed (C2, r_{av}= 0.175±0.047, n=6 axons). (D) Vesicular release probability (vP_r) has a strong negative correlation with paired-pulse ratio at the synapses of a single axon (D1, sample experiment). The set of r-values obtained over all experiments (D2, r_{av}= 0.661±0.070, n=6 axons) demonstrated a significant increase in the strength of the correlation when compared to the P_r-PPR correlations in A2 (paired t-test, $p<0.01$). All data shown is from the same set of 6 experiments, and the sample experiment (A1, B1, C1, D1) depicts all correlations at the same set of synapses along one axon

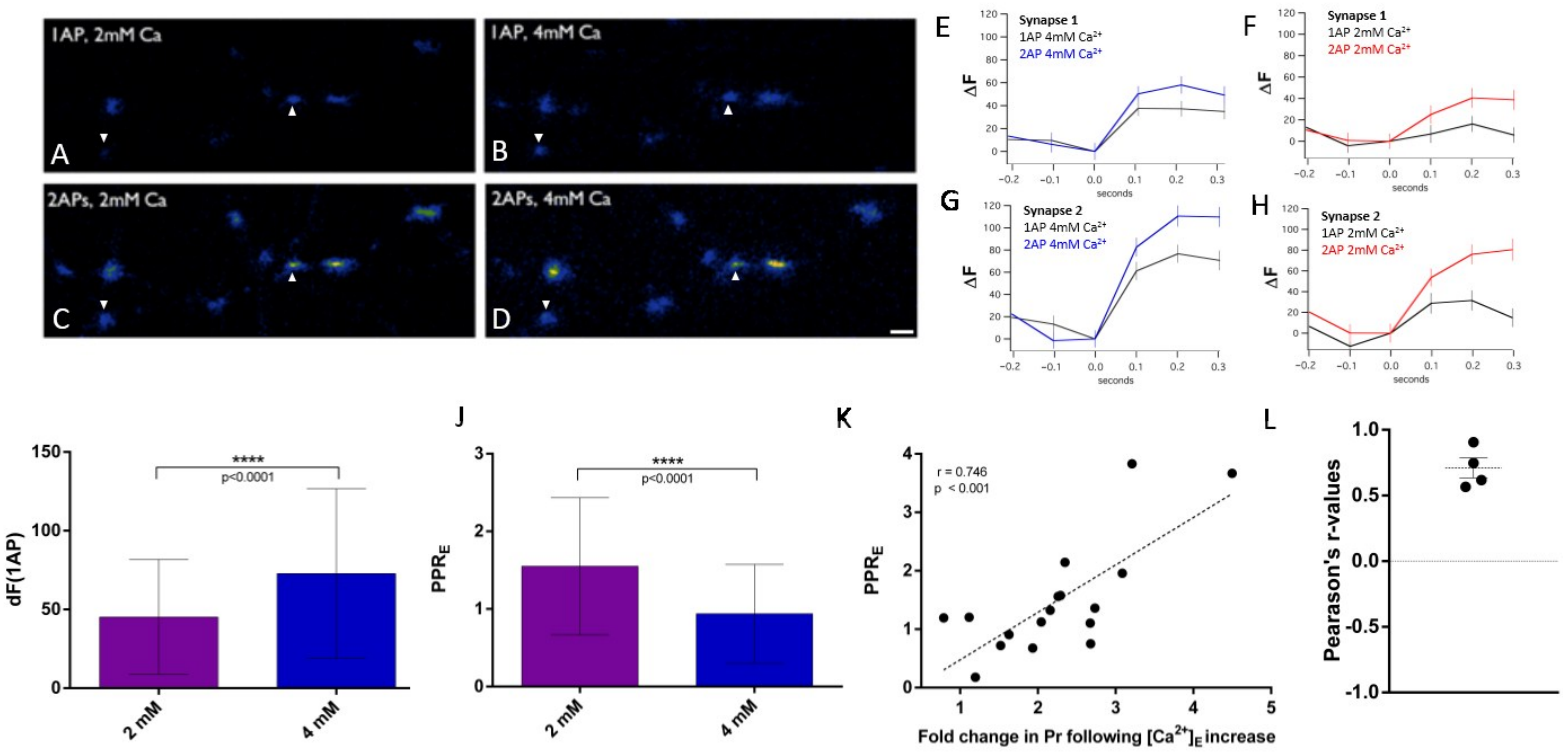

FIGURE 4. Paired-pulse ratio and calcium sensitivity are related at individual synapses. A single axon transfected with sypHl shows fluorescent responses to single stimuli (A-B) and pairs of stimuli (C-D) at individual synapses in both 2 mM (A,C) and 4 mM (B,D) extracellular calcium. Scale bar is 2 μm. (E-H) Traces depict ΔF(1AP) in 2 mM calcium (F & H, black trace) and 4 mM calcium (E & G, black trace) or ΔF(2AP) in 2 mM calcium (red traces) or 4mM calcium (blue traces) at the synapses labelled with white arrowheads (E, F) A synapse with low release probability in 2mM calcium (ΔF(1AP) = 6.64, averaged over 100 trials) shows a large increase in ΔF(1AP) following a change in calcium concentration (fold increase = 4.49). The same synapse shows a high degree of paired-pulse facilitation (PPR_E=3.66) (G, H) A synapse with high release probability in 2mM calcium (ΔF(1AP) = 24.53, averaged over 100 trials) shows a lesser increase in ΔF(1AP) following a change in calcium concentration (fold increase = 1.19).

The same synapse demonstrates reduced facilitation (PPR_E=0.18) (I) ΔF(1AP) in 4mM calcium was significantly larger than ΔF(1AP) in 2mM calcium (Wilcoxon matched-pairs test). (J) Paired-pulse ratio was significantly reduced in 4mM calcium (paired t-test). (K) Calcium sensitivity was assessed using a ratio of ΔF(1AP) in 4 mM calcium to ΔF(1AP) in 2 mM calcium, representing the fold increase in release probability following an increase in extracellular calcium concentration. The ratio is significantly positively correlated with paired-pulse ratio (in 2 mM calcium) at the synapses along a single axon. (L) Summary of correlations between calcium sensitivity and paired-pulse ratio for all experiments (n=4) with error reported as SEM.

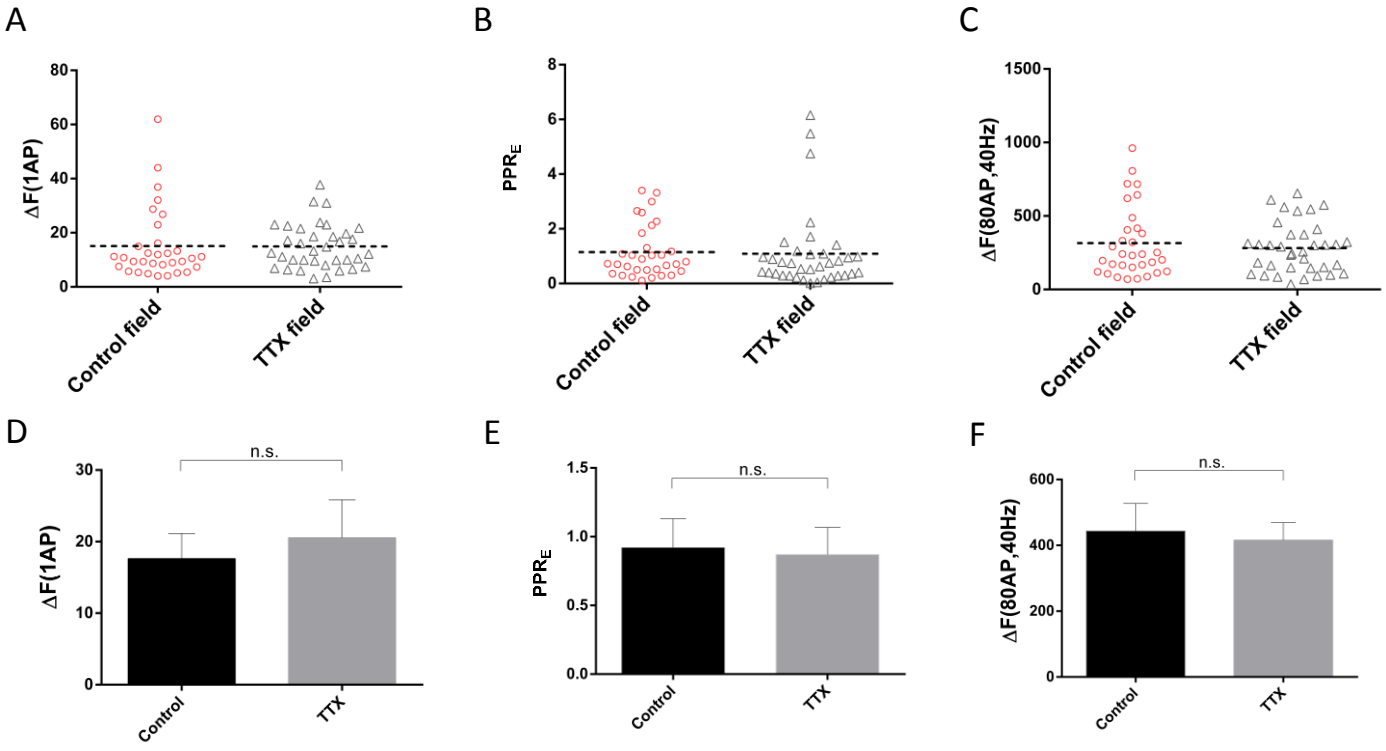

FIGURE 5. Chronic activity suppression with TTX does not influence release probability, PPR, or RRP size. (A-C) Scatter plots comparing (A) fluorescence changes to isolated stimuli as measure of Pr, (B) paired-pulse ratios, and (C) responses to 80 stimuli at 40 Hz as measure of RRP size from synapses in a single TTX-incubated culture to those in a single control culture. (D-F) Summary data over all experiments (n_{TTX}=6, n_{CTRL}=6). There was no significant difference in ΔF(1AP), PPR, or RRP size between groups (unpaired t-test).

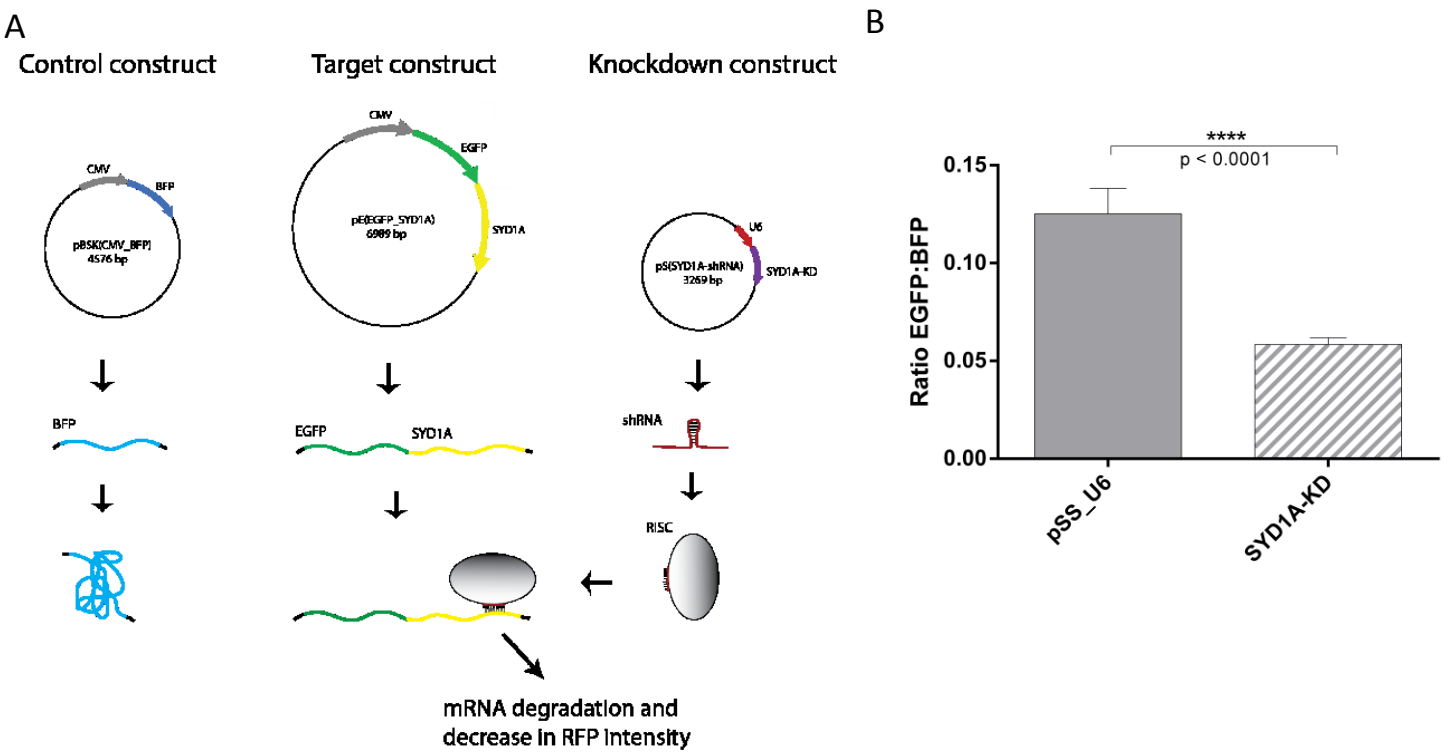

FIGURE 6. Transfection of an shRNA knockdown construct reduces the expression of mSYD1A. (A) A schematic illustrating the test of knockdown efficiency. All neurons were transfected with an EGFP-tagged SYD1A construct and a cytosolic TAG-BFP protein. Fluorescence intensity was measured at segments chosen along 2-3 axons in each field (n_{KD}=36 fields, n_{CTRL}=37 fields). In cells that were also transfected with a knockdown construct, shRNA interferes with protein expression through the degradation of mSYD1A. This reduces the level of EGFP fluorescence, but does not affect the level of BFP fluorescence. (B) There was a 54% decrease in mSYD1A expression in neurons expressing the knockdown construct compared to control neurons (unpaired t-test).

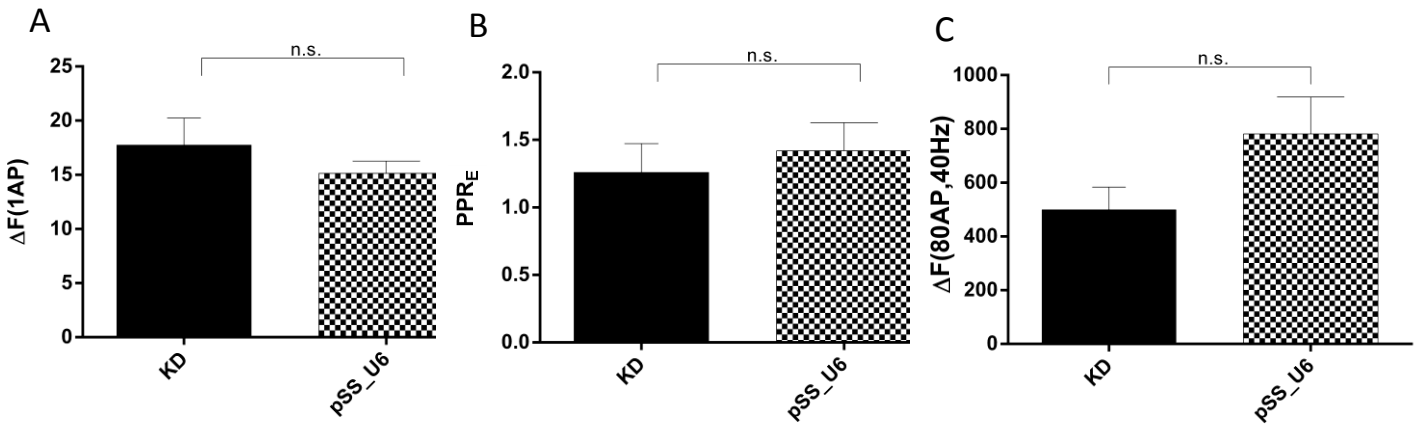

FIGURE 7. SYD1A knockdown has no effect on release probability, PPR, or RRP size. (A) Summary data shows no significant difference in ΔF(1AP) between axons expressing SYD1A-KD (n_{KD}=6) and those expressing the same vector but lacking the knockdown sequence (n_{CTRL}=6). For the same set of axons, there was also no significant difference in (B) PPR or (C) RRP size between groups (unpaired t-tests).

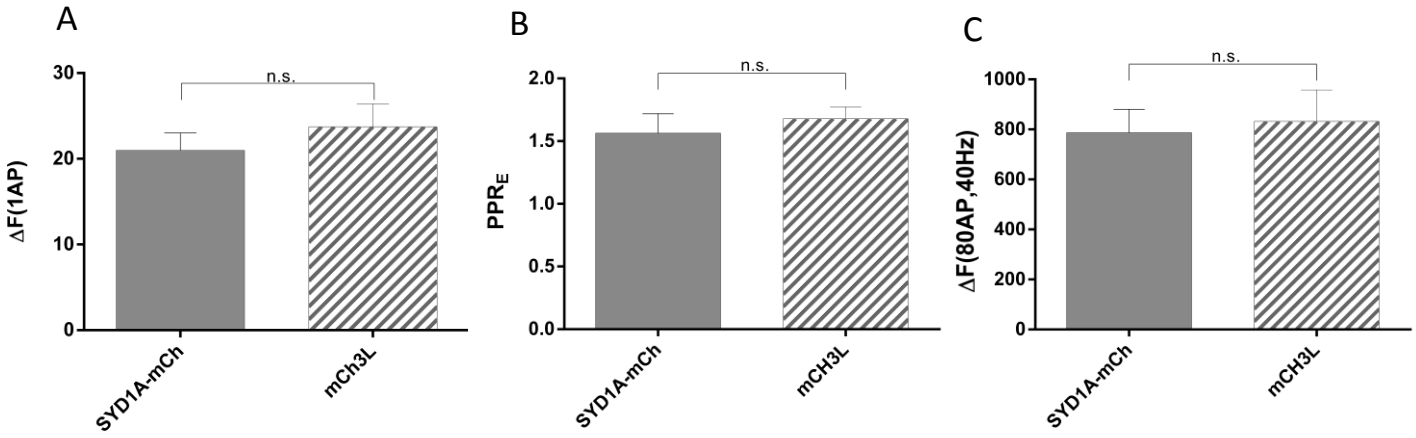

FIGURE 8. SYD1A-mCherry overexpression has no effect on release probability, PPR, or RRP size. (A) Summary data show no significant difference in ΔF(1AP) between axons expressing SYD1A-mCherry (n_{SYD}=10) and those expressing solely mCherry. (n_{CTRL}=10). For the same set of axons, there was also no significant difference in (B) PPR or (C) RRP size between groups (unpaired t-tests).

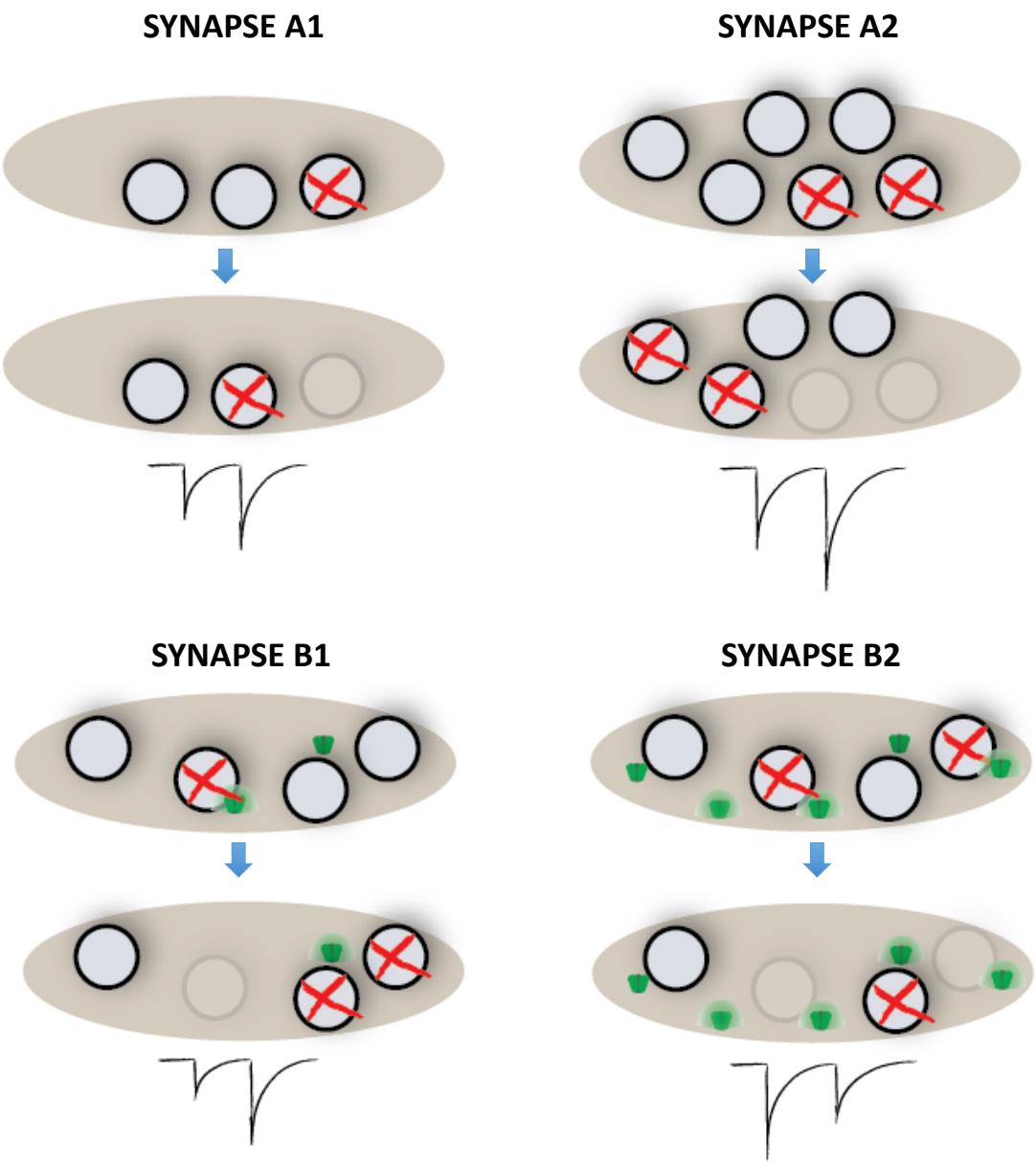

FIGURE 9. Mechanisms regulating vesicular release probability may inversely modulate release probability and PPR, whereas processes altering the size of the RRP may change release probability without altering PPR. The size of the RRP influences the release probability of a synapse at rest. Two synapses with largely different

RRP sizes (A1 and A2) will demonstrate differences in Pr. PPR depends on the proportion of the increase in release probability between stimuli and may therefore be equal if the synapses have similar vesicular release probabilities. Vesicular release probability may be dependent on mechanisms that regulate calcium influx, such as calcium channel density and conductance, or the spatial coupling of vesicles and calcium channels. Two synapses with largely different vesicular release probabilities (represented in this schematic as a difference in channel density between B1 and B2) will have differences in the release probability of the synapse. The synapse with low vesicular release probability tends to facilitate with repeated stimulation as residual calcium increases vesicular release probabilities, e.g. due to saturation of endogenous calcium buffers. At the synapse with high vesicular release probability, the effect of RRP depletion dominates over any effect residual calcium has on vPr, leading to short-term depression.